# Chapter 9
# Genotype by Environment Interaction

Genotype by environment interaction represents a situation where the same QTL varies in size or in sign across different environments. When data are collected from multiple environments, simply taking the average value of the phenotypes across multiple environments will only be able to detect the main effects of QTL. The QTL with interaction effects will have very low power to be detected, especially when the QTL effects across multiple environments are different in sign. Therefore, proper statistical models are required to handle multiple environment data. Zhao and Xu (2012a, b) proposed a multiple QTL model for GxE interaction where all QTL effects are included in the same model. The method is optimal because of the multiple QTL nature. However, it is too advanced to be understood by the majority of the QTL mapping community. Therefore, I will introduce a simple version of the GxE interaction model that utilizes the genome scanning approach. This method adopts the linear mixed model from GWAS by controlling polygenic background via a marker inferred kinship matrix. The method is similar to the meta-analysis in GWAS, but it analyzes data of all environments simultaneously in a single model for the target loci.

Let $y_{ji}$ be the phenotypic value of the *j*th line (individual) collected from the *i*th environment for $j = 1, \cdots, n$ and $i = 1, \cdots, r$, where *n* is the number of lines (sample size) and *r* is the number of environments. In matrix notation, let $y_i = \begin{bmatrix} y_{1i} & y_{2i} & \cdots & y_{ni} \end{bmatrix}^T$ be an $n \times 1$ vector of phenotypic values from all *n* individuals measured in the *i*th environment. Let $Z_k = \begin{bmatrix} Z_{1k} & Z_{2k} & \cdots & Z_{nk} \end{bmatrix}^T$ be the genotype indicators for marker *k* of all *n* individuals. For simplicity, we used $r = 3$ environments as an example to demonstrate the model. The linear mixed model for phenotypic values from the three environments is

$$\begin{bmatrix} y_1 \\ y_2 \\ y_3 \end{bmatrix} = \begin{bmatrix} 1_n & 0 & 0 \\ 0 & 1_n & 0 \\ 0 & 0 & 1_n \end{bmatrix} \begin{bmatrix} \beta_1 \\ \beta_2 \\ \beta_3 \end{bmatrix} + \begin{bmatrix} Z_k \\ Z_k \\ Z_k \end{bmatrix} \gamma_k + \begin{bmatrix} Z_k & 0 & 0 \\ 0 & Z_k & 0 \\ 0 & 0 & Z_k \end{bmatrix} \begin{bmatrix} \delta_{1k} \\ \delta_{2k} \\ \delta_{3k} \end{bmatrix} + \begin{bmatrix} \xi_1 \\ \xi_2 \\ \xi_3 \end{bmatrix} + \begin{bmatrix} e_1 \\ e_2 \\ e_3 \end{bmatrix}$$

where $1_n$ is a unity vector with *n* elements, $\beta_i$ is the mean value of the phenotype in the *i*th environment (fixed effect), $\gamma_k$ is the main effect of marker *k* (fixed effect), $\delta_{ik}$ is the environment specific effect of marker *k* from the *i*th environment (random effect), $\xi_i = \begin{bmatrix} \xi_{1i} & \xi_{2i} & \cdots & \xi_{ni} \end{bmatrix}^T$ is a vector of polygenic effects for all lines in the *i*th environment (random effect) and $e_i = \begin{bmatrix} e_{1i} & e_{2i} & \cdots & e_{ni} \end{bmatrix}^T$ is a vector of residual errors for the *i*th environment.

The random effect $\delta_k = \begin{bmatrix} \delta_{1k} & \delta_{2k} & \delta_{3k} \end{bmatrix}^T$ is assumed to be $N(0, I\tau_k^2)$ distributed, where $\tau_k^2$ is the variance of the effects of marker *k* across environments and represents the GxE interaction effect of locus *k*. The polygenic effects of the three environments are assumed to be multivariate normal with

$$\mathrm{E}\begin{bmatrix}\xi_1\\ \xi_2\\ \xi_3\end{bmatrix}=\begin{bmatrix}0\\ 0\\ 0\end{bmatrix} \text{ and } \mathrm{var}\begin{bmatrix}\xi_1\\ \xi_2\\ \xi_3\end{bmatrix}=\begin{bmatrix}K\phi_1^2 & K\phi_{12} & K\phi_{13}\\ K\phi_{12} & K\phi_2^2 & K\phi_{23}\\ K\phi_{13} & K\phi_{23} & K\phi_3^2\end{bmatrix}$$

where $\phi_i^2$ is the polygenic variance of environment *i*, $\phi_{ii'}$ is the polygenic covariance between environments *i* and $i'$, and *K* (an $n\times n$ matrix) is a marker inferred kinship matrix for all *n* lines calculated based on

$$K=\frac{1}{d}\sum_{k=1}^{m}Z_kZ_k^T$$

where $d=\mathrm{tr}(\sum_{k=1}^{m}Z_kZ_k^T)/n$ is a normalization factor.

The residual errors of the three environments are assumed to be multivariate normal with

$$\mathrm{E}\begin{bmatrix}e_1\\ e_2\\ e_3\end{bmatrix}=\begin{bmatrix}0\\ 0\\ 0\end{bmatrix} \text{ and } \mathrm{var}\begin{bmatrix}e_1\\ e_2\\ e_3\end{bmatrix}=\begin{bmatrix}I\sigma_1^2 & I\sigma_{12} & I\sigma_{13}\\ I\sigma_{12} & I\sigma_2^2 & I\sigma_{23}\\ I\sigma_{13} & I\sigma_{23} & I\sigma_3^2\end{bmatrix}$$

where $\sigma_i^2$ is the residual variance of environment *i*, $\sigma_{ii'}$ is the residual covariance between environments *i* and $i'$.

Let us define

$$\phi=\begin{bmatrix}\phi_1^2 & \phi_{12} & \phi_{13}\\ \phi_{12} & \phi_2^2 & \phi_{23}\\ \phi_{13} & \phi_{23} & \phi_3^2\end{bmatrix} \text{ and } \sigma=\begin{bmatrix}\sigma_1^2 & \sigma_{12} & \sigma_{13}\\ \sigma_{12} & \sigma_2^2 & \sigma_{23}\\ \sigma_{13} & \sigma_{23} & \sigma_3^2\end{bmatrix}.$$

The polygenic covariance matrix and the residual error covariance matrix are $\mathrm{var}(\xi)=\phi\otimes K$ and $\mathrm{var}(e)=\sigma\otimes I$, respectively, where $\otimes$ represents Kronecker matrix product. Let $y=\begin{bmatrix}y_1^T & y_2^T & y_3^T\end{bmatrix}^T$ be the trait values for all lines from all environments. Let $\beta=\begin{bmatrix}\beta_1 & \beta_2 & \beta_3\end{bmatrix}^T$ be the mean values of the three environments. Further define

$$X=\begin{bmatrix}1_n & 0 & 0\\ 0 & 1_n & 0\\ 0 & 0 & 1_n\end{bmatrix},\ U_k=\begin{bmatrix}Z_k\\ Z_k\\ Z_k\end{bmatrix} \text{ and } W_k=\begin{bmatrix}Z_k & 0 & 0\\ 0 & Z_k & 0\\ 0 & 0 & Z_k\end{bmatrix}$$

The linear mixed model can be written in the following compact form,

$$y=X\beta+U_k\gamma_k+W_k\delta_k+\xi+e \tag{1}$$

The expectation of the model is

$$\mathrm{E}(y)=X\beta+U_k\gamma_k \tag{2}$$

and the variance is

$$\mathrm{var}(y)=V=W_kW_k^T\tau_k^2+\phi\otimes K+\sigma\otimes I \tag{3}$$

The restricted maximum likelihood (REML) can bed to estimate the variance and covariance components. These estimated variance covariance components are then used to estimate the fixed effects and to perform statistical tests.

To implement the REML method, the covariance structure should be reformatted as follows,

$$W_k W_k^T \tau_k^2 = \begin{bmatrix} Z_k Z_k^T & 0 & 0 \\ 0 & Z_k Z_k^T & 0 \\ 0 & 0 & Z_k Z_k^T \end{bmatrix} \tau_k^2 \tag{4}$$

$$\begin{aligned} \phi \otimes K = & \begin{bmatrix} K & 0 & 0 \\ 0 & 0 & 0 \\ 0 & 0 & 0 \end{bmatrix} \phi_1^2 + \begin{bmatrix} 0 & 0 & 0 \\ 0 & K & 0 \\ 0 & 0 & 0 \end{bmatrix} \phi_2^2 + \begin{bmatrix} 0 & 0 & 0 \\ 0 & 0 & 0 \\ 0 & 0 & K \end{bmatrix} \phi_3^2 \\ & + \begin{bmatrix} 0 & K & 0 \\ K & 0 & 0 \\ 0 & 0 & 0 \end{bmatrix} \phi_{12} + \begin{bmatrix} 0 & 0 & K \\ 0 & 0 & 0 \\ K & 0 & 0 \end{bmatrix} \phi_{13} + \begin{bmatrix} 0 & 0 & 0 \\ 0 & 0 & K \\ 0 & K & 0 \end{bmatrix} \phi_{23} \end{aligned} \tag{5}$$

$$\begin{aligned} \sigma \otimes K = & \begin{bmatrix} I & 0 & 0 \\ 0 & 0 & 0 \\ 0 & 0 & 0 \end{bmatrix} \sigma_1^2 + \begin{bmatrix} 0 & 0 & 0 \\ 0 & I & 0 \\ 0 & 0 & 0 \end{bmatrix} \sigma_2^2 + \begin{bmatrix} 0 & 0 & 0 \\ 0 & 0 & 0 \\ 0 & 0 & I \end{bmatrix} \sigma_3^2 \\ & + \begin{bmatrix} 0 & I & 0 \\ I & 0 & 0 \\ 0 & 0 & 0 \end{bmatrix} \sigma_{12} + \begin{bmatrix} 0 & 0 & I \\ 0 & 0 & 0 \\ I & 0 & 0 \end{bmatrix} \sigma_{13} + \begin{bmatrix} 0 & 0 & 0 \\ 0 & 0 & I \\ 0 & I & 0 \end{bmatrix} \sigma_{23} \end{aligned} \tag{6}$$

Note that there are 13 variance and covariance components (7 for polygenic effects and 6 for residual errors). Therefore, the covariance structure can be expressed as

$$V = \sum_{l=1}^{13} V_l \theta_l \tag{7}$$

which is a linear combination of all 13 variance-covariance components. If the MIXED procedure in SAS is used, the covariance structure is specified in the REPEATED statement as

```
repeated / subject = intercept type = lin(13) ldata=kk
```

where kk is a matrix with 13*n* rows and *n* + 2 columns to store the 13 structural matrices. Details of the structure matrices are described in an example shown later.

To test the main effects, we first need to estimate the fixed effects using

$$\begin{bmatrix} \hat{\beta} \\ \hat{\gamma}_k \end{bmatrix} = \begin{bmatrix} X^T V^{-1} X & X^T V^{-1} U_k \\ U_k^T V^{-1} X & U_k^T V^{-1} U_k \end{bmatrix}^{-1} \begin{bmatrix} X^T V^{-1} y \\ U_k^T V^{-1} y \end{bmatrix} \tag{8}$$

Let

$$\begin{bmatrix} C_{11} & C_{12} \\ C_{21} & C_{22} \end{bmatrix} = \begin{bmatrix} X^T V^{-1} X & X^T V^{-1} U_k \\ U_k^T V^{-1} X & U_k^T V^{-1} U_k \end{bmatrix}^{-1} \tag{9}$$

The variance of $\hat{\gamma}_k$ is $\text{var}(\hat{\gamma}_k) = C_{22}$. Therefore, the null hypothesis of $H_0 : \gamma_k = 0$ can be tested using the Wald test

$$\text{Wald} = \frac{\hat{\gamma}_k^2}{\text{var}(\hat{\gamma}_k)} = \hat{\gamma}_k^T C_{22}^{-1} \hat{\gamma}_k \tag{10}$$

To test the null hypothesis $H_0 : \tau_k^2 = 0$, i.e., the absence of GxE interaction, we use the likelihood ratio test,

$$\lambda_k = -2\left[ L(\hat{\phi}, \hat{\sigma}) - L(\hat{\tau}_k^2, \hat{\phi}, \hat{\sigma}) \right]$$

where $L(\hat{\tau}_k^2, \hat{\phi}, \hat{\sigma})$ is the restricted log likelihood function evaluated at the MLE of the parameters under the full model and $L(\hat{\phi}, \hat{\sigma})$ is the restricted log likelihood function at the MLE of the parameters under the null model ($\tau_k^2 = 0$).

In the above model, we treated the GxE interaction effects as random. When the number of environments is large, this treatment is advantageous. However, if the number of environments is small, it is more convenient to treat the interaction effects as fixed. The model remains the same,

$$y = X\beta + U_k \gamma_k + W_k \delta_k + \xi + e \tag{11}$$

but the expectation is

$$\text{E}(y) = X\beta + U_k \gamma_k + W_k \delta_k \tag{12}$$

and the variance is

$$\text{var}(y) = V = \phi \otimes K + \sigma \otimes I \tag{13}$$

The null hypothesis for the main effects is $H_0 : \gamma_k = 0$ and the null hypothesis for the GxE interaction effects is $H_0 : \delta_k = 0$. Both hypotheses can be tested using the Wald test statistics,

$$W_{\text{main}} = \hat{\gamma}_k^T C_{22}^{-1} \hat{\gamma}_k$$

and

$$W_{\text{GxE}} = \hat{\delta}_k^T C_{33}^{-1} \hat{\delta}_k$$

where

$$\begin{bmatrix} \hat{\beta} \\ \hat{\gamma}_k \\ \hat{\delta}_k \end{bmatrix} = \begin{bmatrix} X^T V^{-1} X & X^T V^{-1} U_k & X^T V^{-1} W_k \\ U_k^T V^{-1} X & U_k^T V^{-1} U_k & U_k^T V^{-1} W_k \\ W_k^T V^{-1} X & W_k^T V^{-1} U_k & W_k^T V^{-1} W_k \end{bmatrix}^{-1} \begin{bmatrix} X^T V^{-1} y \\ U_k^T V^{-1} y \\ W_k^T V^{-1} y \end{bmatrix} \tag{14}$$

and

$$\begin{bmatrix} C_{11} & C_{12} & C_{13} \\ C_{21} & C_{22} & C_{23} \\ C_{31} & C_{32} & C_{33} \end{bmatrix} = \begin{bmatrix} X^T V^{-1} X & X^T V^{-1} U_k & X^T V^{-1} W_k \\ U_k^T V^{-1} X & U_k^T V^{-1} U_k & U_k^T V^{-1} W_k \\ W_k^T V^{-1} X & W_k^T V^{-1} U_k & W_k^T V^{-1} W_k \end{bmatrix}^{-1} \tag{15}$$

Under the null hypothesis, $W_{\text{main}}$ follows a chi-square with one degree of freedom and $W_{\text{GxE}}$ follows a chi-square distribution with $r-1$ degrees of freedom, where *r* is the number of environments.

**An example in hybrid rice**

We now use an IMF2 hybrid population as an example to demonstrate QTL mapping for GxE interaction. The data have 278 hybrids replicated in two years (1998 and 1999). Therefore, the sample size $n=278$ and the number of environments is $r=2$. We analyzed the KGW trait. The number of markers is 1619, from which we calculated an $n\times n$ kinship matrix. We only demonstrate the GxE analysis for the first marker (bin1). The combined data of phenotypes and genotypes are stored in an excel spread document called "IMF2-phe.csv". The covariance structures are stored in a file called "IMF2-kk.csv" under the full model and a file called "IMF2-kk0.csv" under the null model. The SAS codes for data import and PROC MIXED are shown below,

```
%let dir=C:\Users\SHXU\Dropbox\My UCR Teaching\GEN 234\Lecture Notes\GxE;
filename kk "&dir\IMF2-kk.csv";
filename kk0 "&dir\IMF2-kk0.csv";
filename imf2 "&dir\IMF2-phe.csv";
proc import datafile=kk out=kk dbms=csv replace;
proc import datafile=kk0 out=kk0 dbms=csv replace;
proc import datafile=imf2 out=imf2 dbms=csv replace;
run;


proc mixed data=imf2 method=reml;
  class year;
  model kgw=bin1 year/noint solution;
  repeated /subject=intercept type=lin(7) ldata=kk;
  parms (1) (1) (1) (0) (1) (1) (0)/lowerb=0,0,0,.,0,0,.;
run;

proc mixed data=imf2 method=reml;
  class year;
  model kgw=bin1 year/noint solution;
  repeated /subject=intercept type=lin(6) ldata=kk0;
  parms (1) (1) (0) (1) (1) (0)/lowerb=0,0,.,0,0,.;
run;
```

Under the full model, the estimated variance and covariance components are

| Covariance Parameter Estimates | | |
|---|---|---|
| **Cov Parm** | **Subject** | **Estimate** |
| **LIN(1)** | **Intercept** | 0.02612 |
| **LIN(2)** | **Intercept** | 2.5547 |
| **LIN(3)** | **Intercept** | 3.2050 |
| **LIN(4)** | **Intercept** | 2.8378 |
| **LIN(5)** | **Intercept** | 0.9859 |
| **LIN(6)** | **Intercept** | 0.7786 |
| **LIN(7)** | **Intercept** | 0.2054 |

The test for the main effect of bin 1 is shown below

| Solution for Fixed Effects | | | | | | |
|---|---|---|---|---|---|---|
| **Effect** | **year** | **Estimate** | **Standard Error** | **DF** | **t Value** | **Pr > \|t\|** |
| **bin1** | | 0.1605 | 0.2297 | 552 | 0.70 | 0.4851 |
| **year** | **1998** | 25.8577 | 0.1282 | 0 | 201.73 | . |
| **year** | **1999** | 24.5935 | 0.1365 | 0 | 180.17 | . |

The log likelihood value under the full model is

| Fit Statistics | |
|---|---|
| **-2 Res Log Likelihood** | 1753.0 |
| **AIC (Smaller is Better)** | 1767.0 |
| **AICC (Smaller is Better)** | 1767.2 |
| **BIC (Smaller is Better)** | 1797.2 |

Under the null model (no GxE interaction), the likelihood value is

| Fit Statistics | |
|---|---|
| **-2 Res Log Likelihood** | 1755.1 |
| **AIC (Smaller is Better)** | 1767.1 |
| **AICC (Smaller is Better)** | 1767.3 |
| **BIC (Smaller is Better)** | 1793.0 |

The likelihood ration test statistic is

$$1755.1 - 1753.0 = 2.1$$

The results show that bin1 has neither main effect nor GxE interaction on the trait KGW of the hybrid rice.

We also treated the GxE interaction effects as fixed and ran PROC mixed. The SAS code and out are shown below,

```
proc mixed data=imf2 method=reml;
  class year;
  model kgw=year bin1 bin1*year/noint solution covb;
  repeated /subject=intercept type=lin(6) ldata=kk0;
  parms (1) (1) (0) (1) (1) (0)/lowerb=0,0,.,0,0,.;
run;
```

The type 3 test statistic table

| Type 3 Tests of Fixed Effects | | | | |
|---|---|---|---|---|
| **Effect** | **Num DF** | **Den DF** | **F Value** | **Pr > F** |
| **year** | 2 | 0 | 20656.2 | . |
| **bin1** | 1 | 551 | 0.75 | 0.3883 |
| **bin1*year** | 1 | 551 | 5.05 | 0.0251 |

shows that the GxE (bin1*year) interaction effect is significant because the p-value is 0.0251. However, if Bonferroni correction is used, the p-value is not sufficiently large to pass that stringent criterion.

# *An expectation and maximization algorithm for estimating* Q × E *interaction effects*

**Fuping Zhao & Shizhong Xu**

**Theoretical and Applied Genetics**
International Journal of Plant Breeding Research

ISSN 0040-5752
Volume 124
Number 8

Theor Appl Genet (2012) 124:1375-1387
DOI 10.1007/s00122-012-1794-x

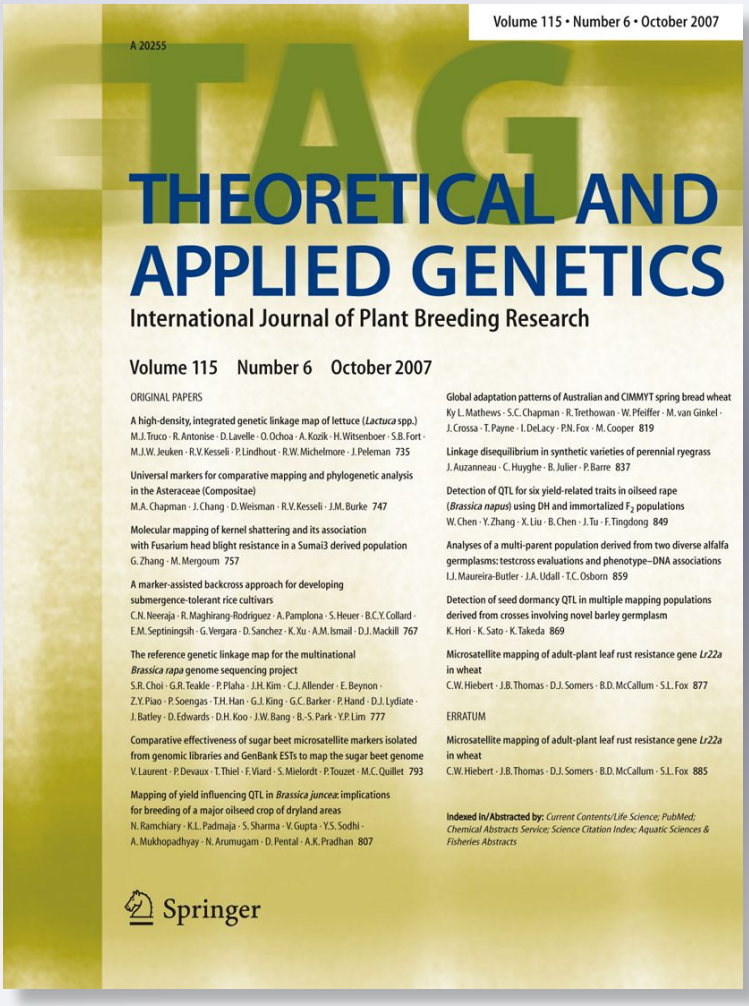


Springer

Theor Appl Genet (2012) 124:1375–1387
DOI 10.1007/s00122-012-1794-x

ORIGINAL PAPER

# An expectation and maximization algorithm for estimating $Q \times E$ interaction effects

**Fuping Zhao · Shizhong Xu**

Received: 20 June 2011 / Accepted: 5 January 2012 / Published online: 2 February 2012


**Abstract** A Markov chain Monte Carlo (MCMC) implemented Bayesian method has been developed to detect quantitative trait loci (QTL) effects and $Q \times E$ interaction effects. However, the MCMC algorithm is time consuming due to repeated samplings of QTL parameters. We developed an expectation and maximization (EM) algorithm as an alternative method for detecting QTL and $Q \times E$ interaction. Simulation studies and real data analysis showed that the EM algorithm produced comparable result as the Bayesian method, but with a speed many magnitudes faster than the MCMC algorithm. We used the EM algorithm to analyze a well known barley dataset produced by the North American Barley Genome Mapping Project. The dataset contained eight quantitative traits collected from 150 doubled-haploid (DH) lines evaluated in multiple environments. Each line was genotyped for 495 polymorphic markers. The result showed that all eight traits exhibited QTL main effects and $Q \times E$ interaction effects. On average, the main effects and $Q \times E$ interaction effects contributed 34.56 and 16.23% of the total phenotypic variance, respectively. Furthermore, we found that whether or not a locus shows $Q \times E$ interaction does not depend on the presence of main effect.

Communicated by M. Sillanpaa.

**Electronic supplementary material** The online version of this article (doi:10.1007/s00122-012-1794-x) contains supplementary material, which is available to authorized users.

F. Zhao · S. Xu (✉)
Department of Botany and Plant Sciences,
University of California, Riverside, CA 92521, USA
e-mail: shizhong.xu@ucr.edu

## Introduction

The mixed model methodology (Henderson 1975) offers an efficient tool for detecting $Q \times E$ interaction for complex quantitative traits with the same set of genotypes measured in multiple environments (Piepho 2000). Under the mixed model framework, we can treat some effects as fixed and others as random, depending on the interpretations of the effects and mathematical convenience of the analysis. Piepho (2000) chose quantitative trait loci (QTL) effects as fixed and environmental effects as random. However, the author used a single marker or interval mapping approach to analyzing the QTL effect and $Q \times E$ interaction. The entire experiment requires multiple analyses with one locus at a time. When multiple QTL are included in a single model, a variable selection scheme may be used because the number of markers can be larger than the sample size. Bayesian shrinkage analysis can handle multiple QTL in a convenient way so that variable selection can be avoided (Xu 2003). In the Bayesian shrinkage analysis, a model can handle many more QTL effects than that can be handled by the traditional maximum likelihood method, even if the number of effects is larger than the sample size. The original Bayesian shrinkage method proposed by Xu (2003) has been applied to QTL mapping within one environment. The method has been extended to mapping $Q \times E$ interaction effects by Chen et al. (2010). The method was implemented via the Markov Chain Monte Carlo (MCMC) algorithm. For any particular marker, the mean of the marker effects across multiple environments represented the main effect and the variance of the marker effects across multiple environments represented the $Q \times E$ interaction effect.

The MCMC-implemented Bayesian method generally provides the highest accuracy of QTL effect estimation, but

is computationally very demanding, especially for large models coupled with large sample sizes. To improve the computational efficiency, Xu (2010) proposed a fast expectation and maximization (EM) algorithm to estimate the posterior modes of variance parameters while the regression coefficients were treated as missing values. This algorithm can also capitalize on valuable information on the basis of prior distribution and is always faster than the MCMC-implemented shrinkage analysis. In this study, we extended the EM algorithm of Xu (2010) to multiple environments for detecting QTL main effects and $Q \times E$ interaction effects.

The doubled-haploid barley data published by Hayes et al. (1993) have been analyzed by numerous investigators (Attari et al. 1998; Fang et al. 2008; Han et al. 1995, 1997; Romagosa et al. 1996; Xu and Hu 2010). They are good sample data for $Q \times E$ interactions because the DH lines were evaluated in multiple environments. The DH population was derived from the cross of "Steptoe" and "Morex", where "Steptoe" is the dominant feed barley in the Northwestern US and "Morex" is the six-row Spring US malting quality standard. There were four agronomic traits (Grain yield, Lodging, Heading date and Height) and four malting quality traits (Grain protein, Alpha amylase, Diastatic power and Malt extract) measured in various numbers of environments. A total of 495 markers were genotyped for 150 DH lines with an average marker interval of 2.23 cM. This dataset was previously analyzed by Hayes et al. (1993) using 123 markers with an average marker density of 9.6 cM. The authors took a least squares approach under the interval mapping scheme for detection of QTL and $Q \times E$ interaction effects (Hayes et al. 1993). However, simultaneous analysis of multiple loci under multiple environments has not been conducted for this barley population. The result of multiple QTL and $Q \times E$ effect analysis should be more informative and can be used to direct further experiments and molecular breeding in barley.

## Methods

### Hierarchical model

The method is developed based on a doubled diploid (DH) design. Let $m$ be the number of environments and $n$ be the number of DH lines. Define $y_j = [y_{j1}\, y_{j2} \cdots y_{jm}]^{\mathrm{T}}$ as an $m \times 1$ vector for the observed phenotypic values of line $j$ measured from the $m$ environments. The linear model for $y_j$ is

$$y_j = \beta + \sum_{k=1}^{q} Z_{jk}\gamma_k + \xi_j \quad (1)$$

where $\beta$ is an $m \times 1$ vector of intercepts, $Z_{jk}$ is a numerically coded genotypic indicator variable for line $j$ at locus $k$, for $k = 1, \ldots, q$, where $q$ is the number of markers, $\gamma_k = [\gamma_{k1}\, \gamma_{k2} \cdots \gamma_{km}]^{\mathrm{T}}$ is an $m \times 1$ vector for the regression coefficients of the phenotypic values on the numerically coded genotype. Note that $\gamma_k$ is a vector and $Z_{jk}$ is a scalar. To model the $Q \times E$ interaction effect, we assume that $\gamma_k$ follows a multivariate normal distribution given below:

$$p(\gamma_k|\alpha_k, \sigma_k^2) = N(\gamma_k|1_m\alpha_k, I_{m\times m}\sigma_k^2) \quad (2)$$

where $1_m$ is a unity vector with dimension $m$, $I_{m\times m}$ is an $m \times m$ identity matrix, $\alpha_k$ is the mean value representing the QTL main effect and $\sigma_k^2$ is the variance of $m$ environment-specific QTL effects represented by vector $\gamma_k$. This variance represents the $Q \times E$ interaction for locus $k$. This type of model with a further modeling on $\gamma_k$ is called the hierarchical model. In the hierarchical model, the first moment parameter $\alpha_k$ is the main effect and the second moment parameter $\sigma_k^2$ represents the degree of $Q \times E$ interaction, called the $Q \times E$ interaction effect in this report. In the multivariate model shown in Eq. 1, the residual error vector $\xi_j = [\xi_{j1}\, \xi_{j2} \cdots \xi_{jm}]^{\mathrm{T}}$ is assumed to be multivariate normal denoted by $\xi_j \sim N(0, \Theta)$, where $\Theta$ is an $m \times m$ variance–covariance matrix. For simplicity, we chose $\Theta = I_{m\times m}\sigma^2$ as the residual variance–covariance structure, called homogenous residual error variance. Other structures are described in the discussion section.

### Prior distribution

We often have enough information from the data to estimate $\beta$ and $\sigma^2$, and thus a uniform prior can be assigned to each of them. The QTL main effect $\alpha_k$ and the $Q \times E$ interaction effect $\sigma_k^2$ are the parameters of interest. The main effect for the $k$th QTL is assigned the following normal prior,

$$p(\alpha_k|\varphi_k^2) = N(\alpha_k|0, \varphi_k^2) \quad (3)$$

where $\varphi_k^2$ is the prior variance. Following Xu (2010) and Yi and Xu (2008), we consider two classes of priors for $\varphi_k^2$. The first class is the scaled inverse Chi-square distribution assigned to $\varphi_k^2$, which is

$$p(\varphi_k^2|\tau_\varphi, \omega_\varphi) = \mathrm{Inv} - \chi^2(\varphi_k^2|\tau_\varphi, \omega_\varphi) \quad (4)$$

A special case of this prior is $(\tau_\varphi, \omega_\varphi) = (-2, 0)$, which is equivalent to the uniform prior $p(\phi_k^2) = 1$. The other special case is $(\tau_\varphi, \omega_\varphi) = (0, 0)$, which represents the Jeffrey's prior, i.e., $p(\varphi_k^2) = 1/\varphi_k^2$. The second class of the priors is the exponential distribution,

$$p(\varphi_k^2|\lambda_\varphi) = \text{Expon}\left(\varphi_k^2|\frac{\lambda_\varphi^2}{2}\right) = \frac{\lambda_\varphi^2}{2}\exp\left(-\frac{\lambda_\varphi^2}{2}\varphi_k^2\right) \quad (5)$$

where $\lambda_\varphi^2$ is the regularization parameter. This exponential prior will result in the Lasso estimation of QTL main effects (Tibshirani 1996), and thus is called the Lasso parameter.

In a similar manner, two different priors are assigned to variance $\sigma_k^2$ (representing the $Q \times E$ interaction). The first prior is the scaled inverse Chi-square prior distribution,

$$p(\sigma_k^2|\tau_\sigma, \omega_\sigma) = \text{Inv} - \chi^2(\sigma_k^2|\tau_\sigma, \omega_\sigma) \quad (6)$$

The second prior is the exponential prior,

$$p(\sigma_k^2|\lambda_\sigma) = \text{Expon}\left(\sigma_k^2|\frac{\lambda_\sigma^2}{2}\right) = \frac{\lambda_\sigma^2}{2}\exp\left(-\frac{\lambda_\sigma^2}{2}\sigma_k^2\right) \quad (7)$$

This exponential prior will lead to the Lasso estimations of environment-specific QTL effects. Note that $(\tau, \omega)$ and $\lambda^2$ are hyper-parameters set up by the investigators. For simplicity, we chose the same hyper-parameters for both $\varphi_k^2$ and $\sigma_k^2$.

## Joint posterior

In the Bayesian shrinkage analysis, the inferences of the parameters are made based on the marginal posterior distributions. The MCMC algorithm can obtain the posterior information of the parameters sampled from the posterior distributions. However, the EM algorithm obtains the posterior modes of the parameters by maximizing the joint density of the posterior. This posterior mode estimation is achieved via an iterative algorithm in lieu of a posterior expectation. The posterior distribution is a combination of the prior and the likelihood. Let $\theta = \{\beta, \sigma^2, \alpha_k, \gamma_k, \varphi_k^2, \sigma_k^2\}$, $\forall k = 1, \ldots, q$, be the parameter vector. The joint posterior distribution of the parameters is expressed as

$$p(\theta|y) = \text{constant} \times p(y|\theta)p(\theta) \quad (8)$$

where

$$p(y|\theta) = \prod_{j=1}^{n} p(y_j|\beta, \gamma, \sigma^2) \quad (9)$$

is the likelihood and

$$p(\theta) = \prod_{k=1}^{q} p(\gamma_k|\alpha_k, \sigma_k^2)p(\alpha_k|\varphi_k^2)p(\sigma_k^2|\theta_\sigma)p(\varphi_k^2|\theta_\varphi) \quad (10)$$

is the prior distribution, where $\theta_\varphi = (\tau_\varphi, \omega_\varphi)$ and $\theta_\sigma = (\tau_\sigma, \omega_\sigma)$ for the scaled inverse Chi-square hyper-parameters, and $\theta_\varphi = \lambda_\varphi^2$ and $\theta_\sigma = \lambda_\sigma^2$ for the exponential hyper-parameters. The density (likelihood) for data $y_j$ is

$$p(y_j|\beta, \gamma, \sigma^2) = N\left(y_j\middle|\beta + \sum_{k=1}^{q} Z_{jk}\gamma_k, \sigma^2\right) \quad (11)$$

The posterior mode estimates of all parameters are obtained by maximizing the log posterior distribution with any quantity involving $\gamma_k$ and $\alpha_k$ replaced by the posterior expectation of that quantity.

## EM algorithm

Derivation of the EM algorithm is straightforward and thus not provided in full length. In this section, we mainly focus on the EM steps by treating $\gamma_k$ and $\alpha_k$ as missing values. We first give the expectation steps and then provide the maximization steps with brief derivation for some key elements.

### *Expectation steps*

The expectation steps involve calculating the posterior expectations and posterior variances of missing values $\gamma_k$ and $\alpha_k$. The conditional posterior for the environment-specific QTL effect $\gamma_k$ is normal with mean and variance specified below. The expectation is

$$E(\gamma_k|\cdots) = \left[\frac{1}{\sigma_k^2}I_{m\times m} + I_{m\times m}\sum_{j=1}^{n} Z_{jk}^2\right]^{-1}\left[\frac{1}{\sigma_k^2}1_m\alpha_k + \sum_{j=1}^{n} Z_{jk}y_j^*\right] \quad (12)$$

where

$$y_j^* = y_j - \beta - \sum_{k'\neq k}^{q} Z_{jk'}\gamma_{k'} \quad (13)$$

are the adjusted phenotypic values of line $j$ by removing all other effects except the effects of locus $k$. The conditional posterior variance of $\gamma_k$ is

$$\text{var}(\gamma_k|\cdots) = \left[\frac{1}{\sigma_k^2}I_{m\times m} + I_{m\times m}\sum_{j=1}^{n} Z_{jk}^2\right]^{-1} \quad (14)$$

The identity matrix $I_{m\times m}$ occurring in the above equation indicates that the expression is an $m \times m$ matrix, rather than a scalar. Similarly, the conditional posterior for $\alpha_k$ is normal with mean and variance given by

$$E(\alpha_k|\cdots) = \left[\frac{1}{\varphi_k^2} + \frac{m}{\sigma_k^2}\right]^{-1}\left[\frac{m}{\sigma_k^2}\sum_{t=1}^{m}\gamma_{jt}\right] \quad (15)$$

and

$$\text{var}(\alpha_k|\cdots) = \left[\frac{1}{\varphi_k^2} + \frac{m}{\sigma_k^2}\right]^{-1} \quad (16)$$

respectively. The conditional posterior means of $\gamma_k$ and $\alpha_k$ are called the shrinkage estimates. Derivation of the shrinkage estimates can be found in Xu (2007).

*Maximization steps*

First, we describe the derivation for the posterior mode of $\sigma_k^2$. The target function for maximization is the expected complete-data log likelihood function. For the scaled inverse Chi-square prior, the part of the expected complete-data log likelihood function relevant to $N_E$ is

$$L(\sigma_k^2|\tau_\sigma,\omega_\sigma) = -\frac{\tau_\sigma+2+m}{2}\ln(\sigma_k^2) - \frac{1}{2\sigma_k^2}\left\{\mathrm{E}\left[(\gamma_k-\alpha_k)^{\mathrm{T}}(\gamma_k-\alpha_k)\right]+\omega_\sigma\right\} \tag{17}$$

Setting $\frac{\partial}{\partial\sigma_k^2}L(\sigma_k^2|\tau_\sigma,\omega_\sigma)=0$ and solving for $\sigma_k^2$, we obtain

$$\sigma_k^2 = \frac{E\left[(\gamma_k-\alpha_k)^{\mathrm{T}}(\gamma_k-\alpha_k)\right]+\omega_\sigma}{\tau_\sigma+2+m} \tag{18}$$

where

$$E\left[(\gamma_k-\alpha_k)^{\mathrm{T}}(\gamma_k-\alpha_k)\right] = E(\gamma_k-\alpha_k)^{\mathrm{T}}E(\gamma_k-\alpha_k) + \mathrm{tr}[\mathrm{var}(\gamma_k|\cdots)] \tag{19}$$

and

$$E(\gamma_k-\alpha_k) = E(\gamma_k|\cdots) - E(\alpha_k|\cdots) \tag{20}$$

For the exponential (Lasso) prior, the part of the expected complete-data log likelihood function relevant to $\sigma_k^2$ is

$$L(\sigma_k^2|\lambda_\sigma) = -\frac{m}{2}\ln(\sigma_k^2) - \frac{E\left[(\gamma_k-\alpha_k)^{\mathrm{T}}(\gamma_k-\alpha_k)\right]}{2\sigma_k^2} - \frac{1}{2}\lambda_\sigma^2\sigma_k^2 \tag{21}$$

Setting $\frac{\partial}{\partial\sigma_k^2}L(\sigma_k^2|\lambda_\sigma)=0$ and solving for $\sigma_k^2$ leads to

$$\sigma_k^2 = \frac{\sqrt{m^2+4\lambda_\sigma^2 E\left[(\gamma_k-\alpha_k)^{\mathrm{T}}(\gamma_k-\alpha_k)\right]}-m}{2\lambda_\sigma^2} \tag{22}$$

The variance component $\varphi_k^2$ is derived using similar approach by maximizing the expected log posterior relevant to $\varphi_k^2$. Under the scaled inverse Chi-square prior, the final expression of the posterior mode is

$$\varphi_k^2 = \frac{E(\alpha_k^2)+\omega_\varphi}{\tau_\varphi+2+1} = \frac{E^2(\alpha_k|\cdots)+\mathrm{var}(\alpha_k|\cdots)+\omega_\varphi}{\tau_\varphi+2+1} \tag{23}$$

For the Lasso prior, we have two solutions with the positive one being

$$\varphi_k^2 = \frac{\sqrt{1+4\lambda_\varphi^2 E(\alpha_k^2)}-1}{2\lambda_\varphi^2} = \frac{\sqrt{1+4\lambda_\varphi^2[E^2(\alpha_k|\cdots)+\mathrm{var}(\alpha_k|\cdots)]}-1}{2\lambda_\varphi^2} \tag{24}$$

Given the updated random effects, let us deal with the fixed effect $\beta$ and the residual error variance $\sigma^2$. The expected complete-data log posterior relevant to $\beta$ and $\sigma^2$ is

$$L(\beta,\sigma^2) = -\frac{mn}{2}\ln\sigma^2 - \frac{1}{2\sigma^2}\sum_{j=1}^{n}E\left[(y_j-\beta-Z_j\gamma)^{\mathrm{T}}(y_j-\beta-Z_j\gamma)\right] \tag{25}$$

Setting $\frac{\partial}{\partial\beta}L(\beta,\sigma^2)=0$ and solving for $\beta$ yields

$$\beta = \frac{1}{n}\sum_{j=1}^{n}\left[y_j - \sum_{k=1}^{q}Z_{jk}E(\gamma_k|\cdots)\right] \tag{26}$$

Finally, we set $\frac{\partial}{\partial\sigma^2}L(\beta,\sigma^2)=0$, solve for $\sigma^2$ and obtain the following solution

$$\sigma^2 = \frac{1}{mn}\sum_{j=1}^{n}E\left[(y_j-\beta-Z_j\gamma)^{\mathrm{T}}(y_j-\beta-Z_j\gamma)\right] \tag{27}$$

where the expectation of the quadratic form, denoted by $E(SS_j)$, has the following expression,

$$E(SS_j) = (y_j-\beta)^{\mathrm{T}}\left[y_j-\beta-\sum_{k=1}^{q}Z_{jk}(E\gamma_k|\cdots)\right] \tag{28}$$

The *E*-steps and *M*-steps are iterated repeatedly until a certain criterion of convergence is reached. At the final iteration, the estimated QTL effect for locus $k$ is denoted by $\hat{\alpha}_k = E(\alpha_k|\cdots)$ and the corresponding variance for the estimate is $S_k^2 = \mathrm{var}(\alpha_k|\cdots)$. Similarly, the estimated environmental specific QTL effect vector is denoted by $\hat{\gamma}_k = E(\gamma_k|\cdots)$ and its variance–covariance matrix is denoted by $V_k = \mathrm{var}(\gamma_k|\cdots)$.

## Hypothesis tests

There are two test statistics for each locus. The main effect QTL is tested under null hypothesis $H_0 : \alpha_k = 0$. The test statistic is the *F*-like statistics denoted by

$$F_k = \frac{\hat{\alpha}_k^2}{S_k^2} \tag{29}$$

The $Q \times E$ interaction effect for locus $k$ is tested under null hypothesis $H_0 : \sigma_k^2 = 0$. Directly testing, this hypothesis is tedious because one has to reanalyze the data

under various reduced models. We reformulated the null hypothesis as $H_0 : \gamma_k = 1\alpha_k$, which is an alternative way of testing $\sigma_k^2 = 0$. The reason for this is that if all elements of vector $\gamma_k$ are equal, we would expect that $\gamma_{k1} = \gamma_{k2} = \cdots = \gamma_{km} = \alpha_k$, and thus $Q \times E$ interaction is absent. We used the Wald statistic (Wald 1943) to test $Q \times E$ interaction,

$$W_k = (\hat{\gamma}_k - 1\hat{\alpha}_k)^{\mathrm{T}} V_k^{-1} (\hat{\gamma}_k - 1\hat{\alpha}_k) \tag{30}$$

Under the null model of $H_0 : \alpha_k = 0$, $F_k$ will approximately follow an $F$-distribution with degrees of freedom 1 and $n$, where $n$ is the sample size. When the sample size is sufficiently large, $F_k$ will be approximated by a Chi-square distribution with one degree of freedom. Under the null model of $H_0 : \gamma_k = 1\alpha_k$ and assuming that $n$ is relatively large, $W_k$ will approximately follow a Chi-square distribution with $m$ degrees of freedom. The critical values of these test statistics for significance declaration can be found from the percentiles of the corresponding central distributions. Alternatively, permutation tests (Churchill and Doerge 1994) may be used to draw empirical thresholds for the test statistics. In our data analysis, we used $\chi^2_{1,1-0.05} = 3.84$ as the critical value for testing the main QTL effect and $\chi^2_{m,1-0.05}$as the critical value for testing $Q \times E$ interaction. We discussed the reason why we did not use the permutation test in the final section of the manuscript.

## Analysis of variances

Although the proportions of trait variance explained by each QTL and each $Q \times E$ interaction may be calculated using the sizes of estimated effects, it is very difficult to compute the overall contributions from all main effect QTL and from all $Q \times E$ interactions due to linkage of multiple QTL. We now use an analysis of variances (ANOVA) approach to partitioning the total phenotypic variance into variance due to all main effect QTL and variance due to all $Q \times E$ interactions. The ANOVA approach was suggested by one of the reviewers. The ANOVA can be accomplished with different analyses under three different models.

1. Full model:

The full model is described as

$$y_j = \beta + \sum_{k=1}^{q} Z_{jk}\gamma_k + \xi_j \tag{31}$$

where $\xi_j \sim N\left(0, I_{m\times m}\sigma_\xi^2\right)$ is the pure residual errors. Note that $\sigma_\xi^2$ is previously denoted by $\sigma^2$. This model facilitates an estimate of the environmental variance using the approach described early.

2. Main effect model:

The model assumes that there is no $Q \times E$ interaction and thus it can be formulated as

$$y_j = \beta + \sum_{k=1}^{q} Z_{jk}1_m\alpha_k + \phi_j \tag{32}$$

where $1_m$ is an $m \times 1$ unity vector and $\phi_j \sim N\left(0, I_{m\times m}\sigma_\phi^2\right)$ is the residual error under the main effect model. Note that both $Z_{jk}$ and $\alpha_k$ are scalars but the model is an $m \times 1$ vector, which explains why a unity vector is inserted there. This model facilitates an estimate of $\sigma_\phi^2$.

3. Null model:

The null model assumes that there is neither QTL main effect nor $Q \times E$ interaction effect for the entire genome. The model only contains an intercept and a residual,

$$y_j = \beta + \zeta_j \tag{33}$$

where $\zeta_j \sim N\left(0, I_{m\times m}\sigma_\zeta^2\right)$ is the residual error under the null model.

We now have three models with three residual error variances. Under the three models, we obtain three estimated variances, $\hat{\sigma}_\xi^2$, $\hat{\sigma}_\varphi^2$ and $\hat{\sigma}_\zeta^2$. In terms of genetic variance components, the three residual variances are expected to be

$$\begin{aligned} E(\hat{\sigma}_\xi^2) &= \sigma_E^2 \\ E(\hat{\sigma}_\phi^2) &= \sigma_E^2 + \sigma_{Q\times E}^2 \\ E(\hat{\sigma}_\zeta^2) &= \sigma_E^2 + \sigma_{Q\times E}^2 + \sigma_Q^2 \end{aligned} \tag{34}$$

where $\sigma_E^2$ is the environmental variance, $\sigma_Q^2$ is the overall variance of main effects and $\sigma_{Q\times E}^2$ is the overall variance of $Q \times E$ interactions. Let $\sigma_P^2 = \sigma_E^2 + \sigma_{Q\times E}^2 + \sigma_Q^2$ be the total phenotypic variance. We are now able to estimate the proportions of phenotypic variance contributed by QTL main effects and $Q \times E$ interaction effects. The two proportions are

$$\hat{H}_Q = \frac{\hat{\sigma}_Q^2}{\hat{\sigma}_P^2} = \frac{\hat{\sigma}_\zeta^2 - \hat{\sigma}_\phi^2}{\hat{\sigma}_\zeta^2} \tag{35}$$

and

$$\hat{H}_{Q\times E} = \frac{\hat{\sigma}_{Q\times E}^2}{\hat{\sigma}_P^2} = \frac{\hat{\sigma}_\phi^2 - \hat{\sigma}_\xi^2}{\hat{\sigma}_\zeta^2} \tag{36}$$

Of course, we can report the so-called broad sense heritability using

$$\hat{H} = \hat{H}_Q + \hat{H}_{Q\times E} = \frac{\hat{\sigma}_Q^2 + \hat{\sigma}_{Q\times E}^2}{\hat{\sigma}_P^2} = \frac{\hat{\sigma}_\zeta^2 - \hat{\sigma}_\xi^2}{\hat{\sigma}_\zeta^2} \tag{37}$$

We have now concluded the methodology development.

## Applications

### Simulated data analysis

We simulated a single large chromosome of 1,120 cM in length covered by 225 codominant markers evenly spaced with 5 cM per marker interval. The simulated population contained $n = 150$ doubled diploid lines evaluated in 16 environments. The genotype indicator variable for line $j$ at locus $k$ was defined as $Z_{jk} = \{1, -1\}$, corresponding to the two genotypes $A_1A_1$ and $A_2A_2$. A total of 10 QTL were simulated with the sizes of the effects and genome locations given in Table 1 and depicted in Fig. 1 for the main effects and Fig. 2 for the $Q \times E$ interaction effects. The environmental error variance was set at $\sigma^2 = 50$. The simulation experiment was replicated 20 times and the average results were reported. In the analysis using the EM algorithm, we chose three different priors: (1) $(\tau, \omega) = (-2, 0)$ corresponding to the uniform prior (denoted by EM-Uniform), (2) $(\tau, \omega) = (0, 0)$ representing the Jeffrey's prior (denoted by EM-Jeffreys) and (3) the Lasso prior (denoted by EM-Lasso) with $\lambda_Q^2 = 1.9446$ and $\lambda_{Q\times E}^2 = 4.9852$. The Lasso parameters were estimated using the empirical formulas $\lambda_Q^2 = \left(\frac{1}{q}\sum_{k=1}^{q}\sigma_k^2\right)^{-\frac{1}{2}}$ for the main effects and $\lambda_{Q\times E}^2 = \left(\frac{1}{q}\sum_{k=1}^{q}\varphi_k^2\right)^{-\frac{1}{2}}$ for the $Q \times E$ interaction effects. The empirical method of choosing the Lasso parameter was proposed by Xu (2010). The same simulated data sets were also analyzed using the MCMC-implemented Bayesian method (Chen et al. 2010) for comparison. In the MCMC analysis, we used the uniform prior for the variance components, i.e., $(\tau, \omega) = (-2, 0)$. The length of the Markov chain contained 60,000 sweeps. The first 30,000 sweeps were deleted as they were considered as observations of the burn-in period. The Markov chain was then thinned at a rate of 1 out of 30. The empirical posterior sample contained 1,000 observations for the post-MCMC analysis. The MCMC experiment for each data analysis was repeated a few times using different seeds to make sure that the chains had converged to the stationary distributions. To test the significance of parameters of interest, we carried out a Bayesian permutation analysis proposed by Che and Xu (2010) to generate the null distributions of the QTL effects, from which an empirical threshold value was obtained for each QTL.

The true main effects and $Q \times E$ interaction effects along with their estimates are summarized in Table 1. Figure 1 depicts the true and estimated effects for QTL and Fig. 2 illustrates the true and estimated $Q \times E$ interaction effects. In terms of closeness of the estimated effects to the true effects, it appeared that the uniform prior of the EM algorithm (EM-Uniform) and MCMC algorithm (also using the uniform prior) produced better estimates than other methods while the MCMC algorithm was superior over the EM algorithm (EM-Uniform). In addition, the EM-Uniform and the MCMC algorithm are capable of separating closely linked QTL and detecting QTL only with main effects or only with $Q \times E$ interaction effects. For example, the second and third QTL had main effects in opposite directions and possessed no $Q \times E$ interaction effects. They were estimated very well by the two algorithms. The sixth QTL possessed $Q \times E$ interaction effect with no main effect. The seventh QTL had main effect only. Both the sixth and the seventh QTL were estimated well by the two algorithms. The Lasso prior produced estimated effects at the corresponding loci simulated, but the values were smaller than the true values, meaning strong shrinkage. The Jeffrey's prior had no power to detect the main effects, but was able to detect $Q \times E$ interaction effects. The failure of Jeffreys' prior for detecting the main effect QTL may be due to the strong shrinkage of the Jeffreys' prior compared to the uniform prior. Nevertheless, all algorithms provided accurate estimates for $\beta$ and $\sigma^2$, which can be found in Table S1 of the Supplemental material.

To validate the analysis of variances for partitioning the total phenotypic variance into variance due to main effect QTL and variance due to $Q \times E$ interaction, we also simulated the data under various reduced models to determine the true $H_Q$ and $H_{Q\times E}$. Although the genetic variances contributed by each QTL and $Q \times E$ interaction can be determined given the true effects, it is hard to determine the overall contributions due to linkage. Therefore, we used a simulation experiment to determine the overall contribution from each source. We simulated two extremely large populations with sample size 10,000 for each population. In the first population, the model was

$$g_j^{\text{full}} = \beta + \sum_{k=1}^{q} Z_{jk}\gamma_k \tag{38}$$

From this population, we calculated the variance of $g_j^{\text{full}}$ across the 10,000 lines. This variance is $\text{var}\left(g_j^{\text{full}}\right) = \sigma_Q^2 + \sigma_{Q\times E}^2$. The second population was simulated under

$$g_j^{\text{main}} = \beta + \sum_{k=1}^{q} Z_{jk}\alpha_k \tag{39}$$

which provided $\text{var}\left(g_j^{\text{main}}\right) = \sigma_Q^2$. The difference between $\text{var}\left(g_j^{\text{full}}\right)$ and $\text{var}\left(g_j^{\text{main}}\right)$ gives the true value of $\sigma_{Q\times E}^2$. Once the true $\sigma_Q^2$, $\sigma_{Q\times E}^2$ and $\sigma_E^2 = 50$ were determined, we obtained $\sigma_P^2$, and thus were able to calculate the proportions of the trait variance contributed by the overall $Q$ and $Q \times E$ interactions. The true proportions and their estimates from the analysis of variances are shown in Table 2.

**Table 1** Simulated QTL main effects and $Q \times E$ interactions effects and their estimated values using the EM algorithms and the MCMC algorithm for 20 replicated simulation experiments

| QTL ID (cM) | Main effect | | | | | $Q \times E$ interaction effects | | | | |
|---|---|---|---|---|---|---|---|---|---|---|
| | True | EM-Uniform | EM-Jeffrey | EM-Lasso | MCMC | True | EM-Uniform | EM-Jeffrey | EM-Lasso | MCMC |
| 1 (45) | 3.1774 | 2.8345 (±0.2391) | 0.0000 (±0.2882) | 1.9382 (±0.2069) | 3.1249 (±0.1440) | 15.6341 | 14.4800 (±0.9766) | 21.7345 (±1.0740) | 7.7508 (±0.3434) | 15.2919 (±1.0813) |
| 2 (245) | −4.1395 | −3.5875 (±0.5201) | 0.0000 (±0.0000) | −1.9538 (±0.4592) | −3.6174 (±0.4185) | 26.3211 | 24.9924 (±2.8046) | 34.3821 (±2.7470) | 10.9568 (±0.7419) | 26.7689 (±2.9756) |
| 3 (250) | 2.6448 | 2.1867 (±0.4364) | 0.0000 (±0.0000) | 1.1357 (±0.3681) | 2.2180 (±0.3549) | 14.0425 | 12.0439 (±1.7527) | 15.5249 (±2.2390) | 6.3680 (±0.6926) | 12.9048 (±1.7973) |
| 4 (395) | 3.1716 | 2.7745 (±0.4364) | 0.0000 (±0.0000) | 2.1647 (±0.3250) | 3.0733 (±0.1350) | 8.8099 | 8.4638 (±0.8013) | 16.279 7 (±1.1059) | 5.2522 (±0.3885) | 9.0920 (±0.8335) |
| 5 (495) | 0.0000 | 0.0000 (±0.0003) | 0.0000 (±0.0000) | −0.0001 (±0.0002) | −0.0365 (±0.1264) | 7.7573 | 7.2245 (±0.6636) | 5.7188 (±2.4093) | 4.4099 (±0.3232) | 7.2557 (±0.8025) |
| 6 (645) | 3.6336 | 3.4824 (±0.3061) | 3.1525 (±0.1645) | 2.5802 (±0.3141) | 3.6894 (±0.2124) | 11.4581 | 10.3164 (±1.1246) | 9.4270 (±1.0923) | 6.1990 (±0.5186) | 10.6544 (±1.1599) |
| 7 (745) | −3.0000 | −2.6982 (±0.3006) | 0.0000 (±0.0000) | −2.4783 (±0.3082) | −2.8449 (±0.1516) | 0.0000 | 0.0192 (±0.0568) | 7.7876 (±0.9004) | 0.0134 (±0.0346) | 0.3463 (±0.1424) |
| 8 (895) | 3.7301 | 3.3775 (±0.2882) | 0.0000 (±0.0000) | 2.6128 (±0.2110) | 3.5734 (±0.1470) | 11.5579 | 10.5296 (±1.1422) | 20.9925 (±1.3359) | 6.3348 (±0.3761) | 11.1971 (±1.1081) |
| 9 (995) | 3.5485 | 2.8452 (±0.4602) | 0.350603 (±0.7177) | 2.7393 (±0.2395) | 3.0400 (±0.6797) | 6.7232 | 5.5139 (±2.5076) | 14.4399 (±3.5960) | 3.9694 (±1.2763) | 6.6532 (±0.9380) |
| 10 (1,095) | 4.4746 | 4.2675 (±0.2728) | 0.0000 (±0.0000) | 3.1905 (±0.3288) | 4.3109 (±0.2082) | 15.3884 | 14.1816 (±1.3672) | 29.5012 (±1.4246) | 7.6920 (±0.5432) | 15.1815 (±1.3665) |

EM-Uniform: $(\tau, \omega) = (-2, 0)$; EM-Jeffrey: $(\tau, \omega) = (0, 0)$; EM-Lasso: $\lambda_Q^2 = 1.9446$ and $\lambda_{Q\times E}^2 = 4.9852$; MCMC-Bayesian method. The standard errors are included in the parentheses. The numbers in parentheses are standard deviations of the estimated effects across the 20 replicated experiments

We can see that the estimated $H_Q$ and $H_{Q\times E}$ were very close to the true proportions.

Our simulation experiments showed that the EM algorithm with the uniform prior and the MCMC-implemented Bayesian method (uniform prior) are optimal in $Q \times E$ detection. The latter had a slight advantage over the former, but the advantage was barely noticeable. The great advantage of the EM algorithm is the fast computational speed. For each dataset, the EM algorithm required an average of 3.4 min of CPU time while the MCMC algorithm took 330.5 min on a desktop with an Inter Core i7-2600 3.4-GHz processor and 4.00 GB RAM (see the last row of Table 2). Therefore, the EM algorithm developed here can be a suitable alternative method for detecting $Q \times E$ interactions. The time consuming MCMC algorithm still has its advantages over the EM algorithm regarding the ability to generate an empirical posterior distribution (shape) for each estimated QTL effect while the EM algorithm only provides the posterior mode and posterior variance for each QTL.

## Real data analysis

We applied the new EM algorithm to analyze the doubled-haploid population published by Hayes et al. (1993). The genotype and phenotype data were retrieved from the following two websites: http://www.genenetwork.org/genotypes/SXM.geno and http://wheat.pw.usda.gov/ggpages/SxM/phenotypes.html.

For the article to be self-contained, we briefly summarized the main features of the data. This dataset consisted of 150 doubled haploids (DH) derived from the cross of two spring barley varieties, Steptoe and Morex, designated as S × M. The traits consisted of three agronomic traits (Grain yield, Heading date and Height) and five malting quality traits (Lodging, Grain protein, Alpha amylase, Diastatic power and Malt extract). As an example, we only presented in detail the result of a malting quality trait named Lodging. This trait was measured in six environment and, therefore, $m = 6$ and $n = 150$. Other traits were also analyzed but results are not presented in detail as we did for Lodging (see Table 4 for all results). The total number of markers was 495 distributed along seven chromosomes of the barley genome. Because of the small sample size, we could not analyze all the 495 markers simultaneously in a single model due to high multi-collinearity. Therefore, we selected one marker in every 5 cM, leaving a total of 225 markers for the entire genome. If a selected genome location did not overlap with a marker, genotypes of the 150 lines were imputed from linked markers using the multipoint method (Jiang and Zeng 1997). The genotype of each marker was coded as +1 for the Steptoe allele and −1 for the Morex allele. All the 225

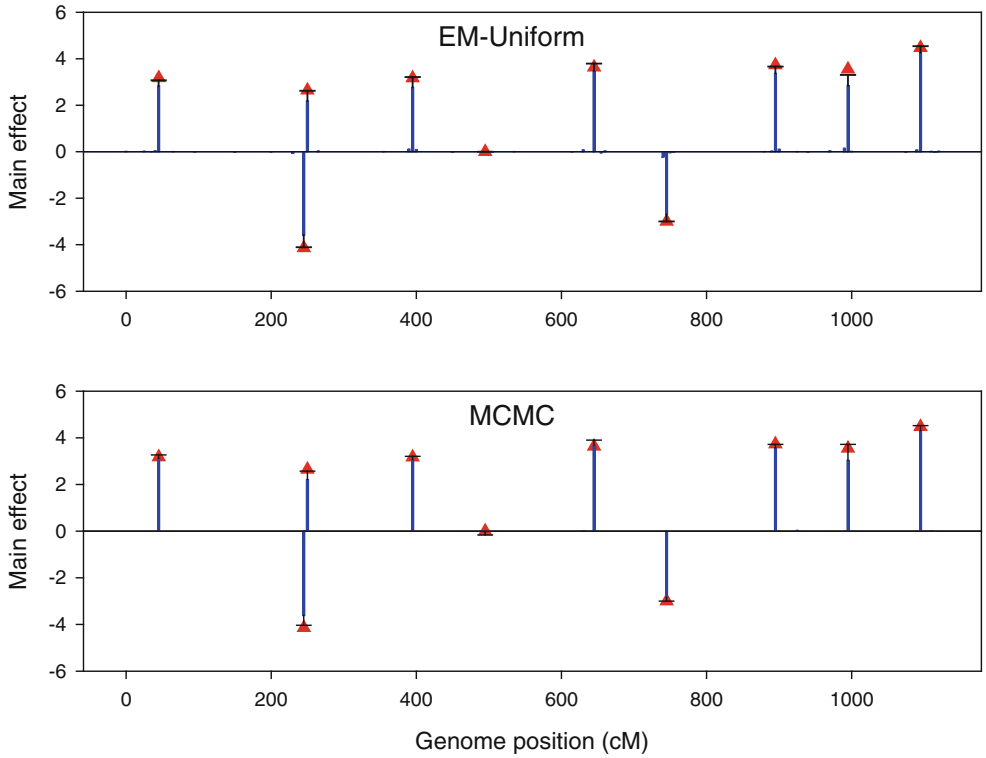


**Fig. 1** True and estimated main effects of QTL plotted against genome location in the simulated data analysis. The red triangles indicate the true effects, the needles in blue show the estimated effects and error bars in black represent the standard errors. The top panel shows the result using the EM-Uniform algorithm and the bottom panel shows the result from the MCMC-implemented Bayesian method

putative loci were evaluated simultaneously in a single model.

We used the EM-Uniform algorithm and the MCMC algorithm to analyze this trait. The estimated QTL main effects are depicted in Fig. 3, where the top panel gives the result of the EM-Uniform and the bottom panel shows the result of the MCMC algorithm. The two methods generated similar results in most chromosome regions except a few places where the MCMC algorithm had extra peaks that were missing from the EM-Uniform algorithm. The major difference comes from the last chromosome where the EM-Uniform algorithm showed one peak but the MCMC algorithm gave two peaks (one overlaps with the one generated from the EM-Uniform algorithm). Another difference between the two methods is that the MCMC algorithm appears to have stronger shrinkage for large QTL but weaker shrinkage for smaller QTL than the EM-Uniform algorithm. The estimated $Q \times E$ interaction effects are depicted in Fig. 4, where the top panel shows the result of the EM-Uniform algorithm and the bottom panel shows that of the MCMC algorithm. Again, the two algorithms generated much the same result. The only difference is that the MCMC algorithm appeared to have spread each $Q \times E$ into a few smaller ones in the neighborhood of the major peak for some unknown reasons.

Result of analysis of variances for the trait Lodging is presented in Table 3. The two methods produced similar results regarding the estimated $H_Q$ and $H_{Q\times E}$. On average, $\hat{H}_Q \approx 0.21$ and $\hat{H}_{Q\times E} \approx 0.31$ leading to an estimated broad sense heritability of $\hat{H} \approx 0.52$. The computational times for the EM-Uniform and MCMC algorithm were 5.20 and 289.05 min, respectively. Again, the advantage of the EM algorithm over the MCMC algorithm is well supported.

The $F$ and $W$ test statistics for the main effects and $Q \times E$ interaction effects for this trait (Lodging) are presented in Fig. 4. The critical value for main effect detection was $\chi^2_{1,0.95} = 3.84$ (one degree of freedom) and the corresponding critical value for $Q \times E$ detection was $\chi^2_{6,0.95} = 12.59$ (six degrees of freedom because there were six environments). Using these critical values, we detected $N_Q = 9$ main effect QTL and $N_{Q\times E} = 10$ interaction effects. Among these loci, $N_{Q\cap Q\times E} = 4$ of them showed both $Q$ and $Q \times E$, and $N_{Q\cup Q\times E} = 9 + 10 - 4 = 15$ was the total number of loci with either $Q$ or $Q \times E$ or both. Among the total number of loci detected, $N_Q/N_{Q\cup Q\times E} = 0.60$ had main effects and $N_{Q\times E}/N_{Q\cup Q\times E} = 0.67$ had $Q \times E$ interaction effects. Among the total number of loci evaluated ($N_{\text{Marker}} = 225$), $N_Q/N_{\text{Marker}} = 0.040$ had main effects and $N_{Q\times E}/N_{\text{Marker}} = 0.044$ had $Q \times E$ effects.

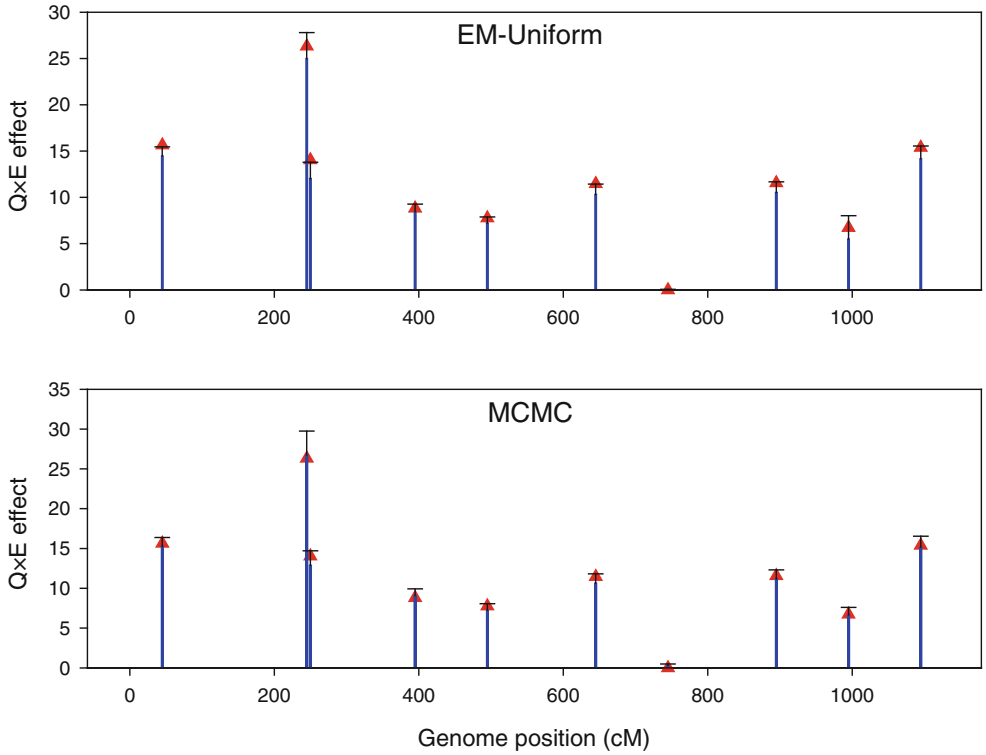


**Fig. 2** True and estimated $Q \times E$ interaction effects plotted against genome location in the simulated data analysis. The red triangles indicate the true effects, the needles in blue show the estimated effects and error bars in black represent the standard errors. The top panel shows the result using the EM-Uniform algorithm and the bottom panel shows the result from the MCMC-implemented Bayesian method

**Table 2** True and estimated proportions of phenotypic variance explained by QTL for the simulated data analysis

| | True value | EM-Uniform | MCMC |
|---|---|---|---|
| Main ($H_Q$) | 0.3546 | 0.3511 (±0.0064) | 0.3534 (±0.0076) |
| $Q \times E$ ($H_{Q\times E}$) | 0.4543 | 0.4682 (±0.0085) | 0.4523 (±0.0090) |
| Computing time[a] | – | 3.40 (±0.5000) | 330.50 (±0.7631) |

[a] The last row gives the computing time in minute for the two algorithms and the standard errors are included in parentheses

The overall proportion of the phenotypic variance contributed by main effects was $H_Q = 0.21$ and the corresponding proportion explained by $Q \times E$ was $H_{Q\times E} = 0.32$. Due to linkage, if two neighboring markers were both significant and in the same directions, we only counted as one. This would correct any upward bias regarding the estimated number of QTL. If a locus had a QTL effect but no $Q \times E$ interaction, but a locus 5 cM away from this locus showed $Q \times E$ interaction, we claimed that the $Q$ and $Q \times E$ were in the same locus.

Finally, we used the EM-Uniform algorithm to analyze the remaining seven traits. Three of the seven traits were replicated in 16 environments and four of them were replicated in nine environments. The results of all trait analysis using the EM-Uniform algorithm (including Lodging measured in six environments) are summarized in Table 4. The number of QTL and $Q \times E$ interactions for the remaining seven traits was calculated using the same rules as we did for the Lodging analysis. For all the eight traits, on average, the proportion of trait variance explained by $Q$ was $H_Q = 0.346$ and the corresponding proportion explained by $Q \times E$ was $H_{Q\times E} = 0.162$. The conclusion was that the main effect QTL played a more important role than the $Q \times E$ interaction effects. Another important discovery from Table 4 was that the number of loci showing both $Q$ and $Q \times E$ was very small with an average of 2.75 across all eight traits. Majority of the loci showed either $Q$ or $Q \times E$ but not both. Table 4 only provides a brief summary of the real data analysis. Detailed information regarding the actual estimated effects and locations of the significant loci are presented in Figures S1–S4 of the Supplemental material.

## Discussion

We developed a hierarchical model for detection of $Q \times E$ interactions implemented via the EM algorithm. We also

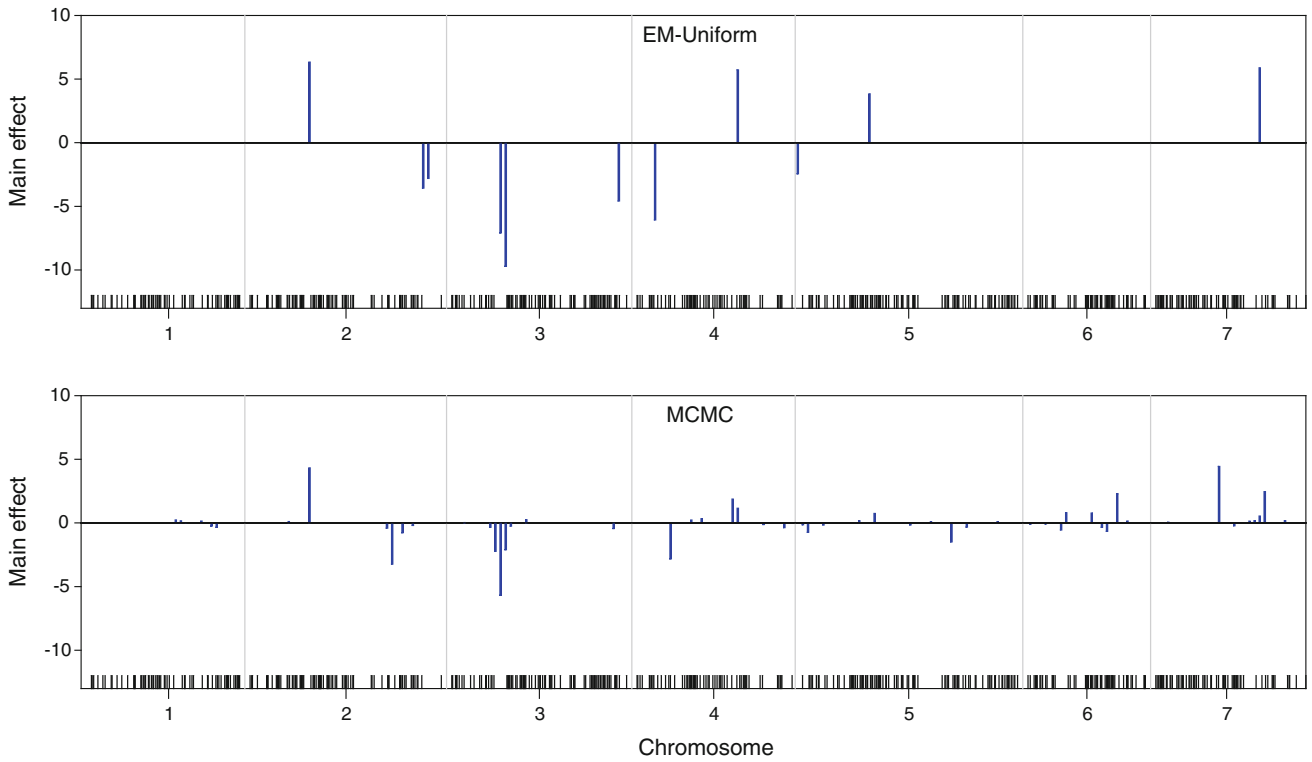


**Fig. 3** Estimated main effects plotted against genome location for trait "Lodging" of the barley data analysis. The top panel shows the result of the EM-Uniform algorithm and the bottom panel shows the result of the MCMC algorithm. The seven chromosomes are separated by the vertical reference lines. The barcode like ticks on the *x*-axis represent the locations of the 495 markers

compared the EM algorithm with the Bayesian method (Chen et al. 2010) for detecting $Q \times E$ interactions. Results of the two methods are similar. The major advantage of the EM algorithm is the fast speed of computation. The Bayesian method, although slow in computation, still shows its advantage because it provides the posterior distribution (shape) for a QTL effect. This allows investigators to draw credibility interval for each estimated QTL effect. The EM algorithm, however, only gives the posterior mode and posterior variance for each QTL effect. Therefore, the EM algorithm is only a suitable alternative for the Bayesian method.

In the original data analysis of Hayes et al. (1993), the authors also reported $Q \times E$ interactions using the interval mapping approach (Haley and Knott 1992; Knapp et al. 1990) by analyzing the data separately with one environment at a time. They evaluated the differences of QTL effects among the environments. The original method is considered an ad hoc method. We examined the $Q \times E$ interaction effects detected from the ad hoc method and compared the results with ours. We found that all effects detected by Hayes et al. (1993) were also detected with our method. In addition, we detected more $Q \times E$ interaction effects (see Figures S1–S4 of the Supplemental material for the results of our analysis using the EM algorithm). This implied that our method may have higher power than the *ad hoc* method.

The hierarchical model presented is considered the simplest model of this kind. The reason is that we assumed $\xi_j \sim N(0, I_{m\times m}\sigma^2)$, which has the simplest residual variance structure. The simplest model seems to work well, as demonstrated in the barley data analysis. Further improvement may be done by incorporating more complicated residual variance structures. We did not do that in this study because (1) the result would be difficult to present and (2) it would be hard to partition the total variance into variance due to QTL main effects and variance due to $Q \times E$ interactions. In the future, we expect to see more experiments with traits measured in multiple environments. In any particular real data analysis, it is worthy to explore complicated error structures. The most advanced variance structure is the factor-analytic structure as given by Chen et al. (2010), in which the $m$ environments are considered to be controlled by a few underlying factors. Extension of our model to factor-analytic structure is possible, although not a simple task. Two other structures are easy to incorporate, which are (1) the heterogeneous variance structure and (2) the fully unstructured variance matrix. The general covariance structure is $\xi_j \sim N(0, \Theta)$ where $\Theta$ is an $m \times m$ matrix. For the heterogeneous

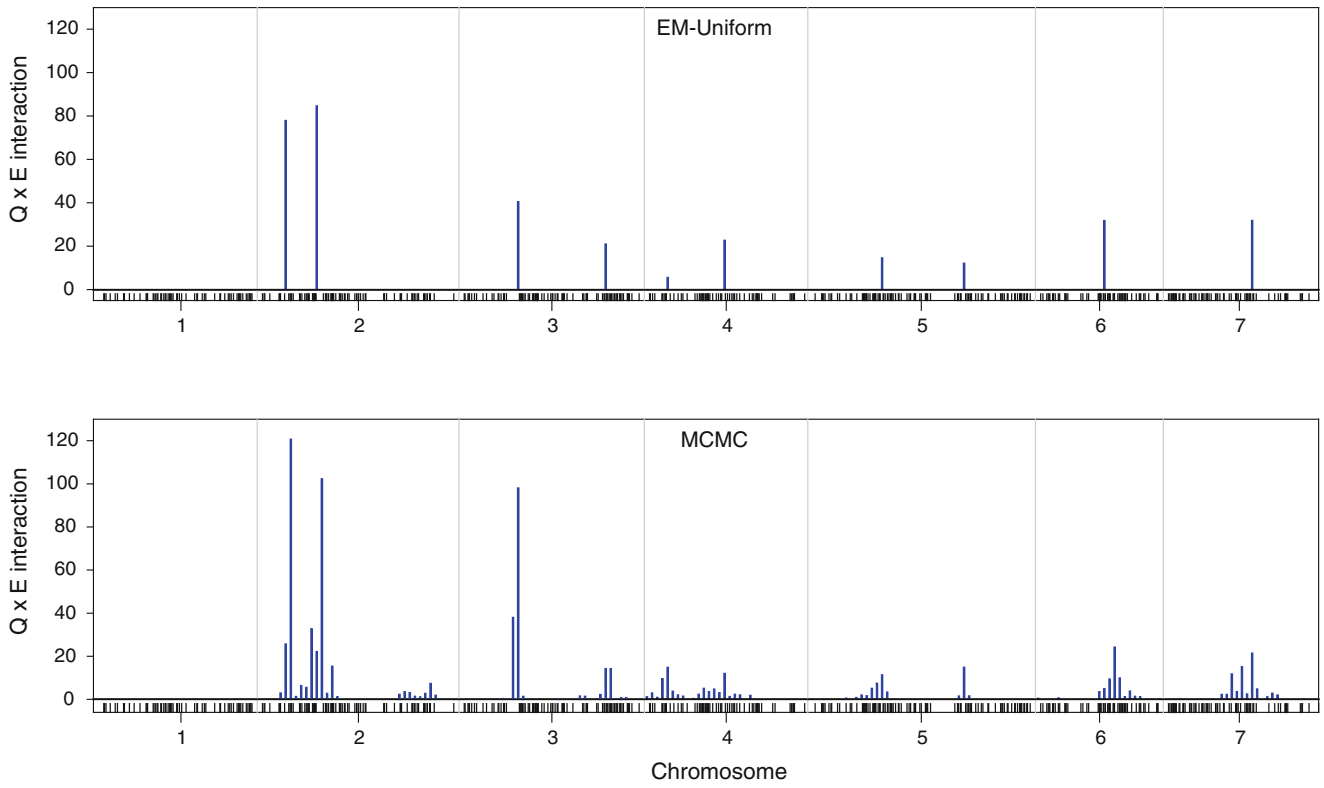


**Fig. 4** Estimated $Q \times E$ interaction effects plotted against genome location for trait "Lodging" of the barley data analysis. The top panel shows the result of the EM-Uniform algorithm and the bottom panel shows the result of the MCMC algorithm. The seven chromosomes are separated by the vertical reference lines. The barcode like ticks on the $x$-axis represent the locations of the 495 markers

**Table 3** Estimated proportions of phenotypic variance explained by QTL for trait Lodging of the barley data analysis

| | EM-Uniform | MCMC |
|---|---|---|
| Main ($H_Q$) | 0.2105 | 0.2297 |
| $Q \times E$ ($H_{Q\times E}$) | 0.3283 | 0.3071 |
| Computing time[a] | 5.20 | 289.05 |

[a] The last row gives the computing time in minute for the two algorithms

residual variance structure, $\Theta = D = \text{diag}\{d_1, \ldots, d_m\}$, where $d_t$ is the variance for the $t$th environment. For the fully unstructured variance matrix, $\Theta = \Sigma$ is a positive definite symmetric matrix. To incorporate these variance structures, we need to replace $I_{m\times m}\sigma^2$ occurred in any place during the derivation of the simple structure by $\Theta$. In addition, the maximization step for $\sigma^2$ is replaced by the maximization step for $D$ using

$$D = \frac{1}{n}\sum_{j=1}^{n} \text{diag}\left\{E\left[\left(y_j - \beta - Z_j\gamma\right)\left(y_j - \beta - Z_j\gamma\right)^{\mathrm{T}}\right]\right\} \quad (40)$$

For the fully unstructured residual variance matrix, we need to replace the maximization step for $\sigma^2$ by the maximization step for $\Sigma$,

$$\Sigma = \frac{1}{n}\sum_{j=1}^{n} E\left[\left(y_j - \beta - Z_j\gamma\right)\left(y_j - \beta - Z_j\gamma\right)^{\mathrm{T}}\right] \quad (41)$$

Note that the transposition operator ($^{\mathrm{T}}$) occurs in the residual vector of the right, different from Eq. (27) in which $^{\mathrm{T}}$ occurred in the left. Chen et al. (2010) found that the $D$ structure can have significant improvement over the simple structure, but the $\Sigma$ structure may have only a marginal improvement. Again, we did not use $D$ because we want to partition $H$ into $H_Q$ and $H_{Q\times E}$, which is not straightforward in situations other than the simple structure.

The hierarchical model involves hyper-parameters $(\tau, \omega)$ for the scaled inverse Chi-square prior and $\lambda^2$ for the Lasso prior. For simplicity, we examined $(\tau, \omega) = (-2, 0)$ and $(\tau, \omega) = (0, 0)$ for the scaled inverse Chi-square prior. The Lasso prior $\lambda^2$ was drawn from the data using the empirical formula of Xu (2010). In real data analysis, these hyper-parameters may be determined by cross-validation analysis. The set of hype-parameters that generate the minimum squared prediction error (PE) should be selected and the results from that set of hyper-parameters should be reported.

Significance test is another issue in $Q \times E$ detection. We used the percentiles of central Chi-square distributions

**Table 4** Summary statistics for eight quantitative traits in the "Steptoe" × "Morex" doubled-haploid barley population analysis using the EM-Uniform algorithm

| | Trait | | | | | | | | Average |
|---|---|---|---|---|---|---|---|---|---|
| | Yield | Lodging | Height | Heading | Grain protein | Alpha amylase | Diastatic power | Malt extract | |
| $N_{\text{Environment}}$ | 16 | 6 | 16 | 16 | 9 | 9 | 9 | 9 | 11.25 |
| $N_Q$ | 18 | 9 | 39 | 32 | 15 | 22 | 26 | 11 | 21.50 |
| $N_{Q\times E}$ | 9 | 10 | 3 | 2 | 3 | 6 | 10 | 5 | 6.00 |
| $N_{Q\cap Q\times E}$ | 3 | 4 | 2 | 2 | 0 | 3 | 7 | 1 | 2.75 |
| $N_{Q\cup Q\times E}$ | 24 | 15 | 40 | 32 | 18 | 25 | 29 | 15 | 24.75 |
| $N_Q/N_{Q\cup Q\times E}$ | 0.7500 | 0.6000 | 0.9750 | 1.0000 | 0.8333 | 0.8800 | 0.8966 | 0.7333 | 0.8335 |
| $N_{Q\times E}/N_{Q\cup Q\times E}$ | 0.3750 | 0.6667 | 0.0750 | 0.0625 | 0.1667 | 0.2400 | 0.3448 | 0.3333 | 0.0956 |
| $N_Q/N_{\text{Marker}}$ | 0.0800 | 0.0400 | 0.1733 | 0.1422 | 0.0667 | 0.0978 | 0.1156 | 0.0489 | 0.0956 |
| $N_{Q\times E}/N_{\text{Marker}}$ | 0.0400 | 0.0444 | 0.0133 | 0.0089 | 0.0133 | 0.0267 | 0.0444 | 0.0222 | 0.0267 |
| $N_{Q\cap Q\times E}/N_{\text{Marker}}$ | 0.0133 | 0.0178 | 0.0089 | 0.0089 | 0.0000 | 0.0133 | 0.0311 | 0.0044 | 0.0122 |
| $H_Q$ | 0.1145 | 0.2105 | 0.5208 | 0.6881 | 0.2335 | 0.3496 | 0.5620 | 0.0856 | 0.3456 |
| $H_{Q\times E}$ | 0.3443 | 0.3283 | 0.1159 | 0.1212 | 0.0833 | 0.0915 | 0.1134 | 0.1006 | 0.1623 |

$N_{\text{Environment}}$, number of environments; $N_{\text{Marker}}$, number of markers; $N_Q$, number of main effects; $N_{Q\times E}$, number of $Q \times E$ interaction effects; $N_{Q\cup Q\times E}$, total number of effects (including $Q$ and $Q \times E$); $N_{Q\cap Q\times E}$, number of loci showing both effects ($Q$ and $Q \times E$ interaction effects); $N_Q/N_{Q\cup Q\times E}$, proportion of the number of main effect to total number of effects; $N_{Q\times E}/N_{Q\cup Q\times E}$, proportion of the number of $Q \times E$ interaction effects to the total number of effects; $N_Q/N_{\text{Marker}}$, proportion of the number of main effects to the total number of markers; $N_{Q\times E}/N_{\text{Marker}}$, proportion of the number of $Q \times E$ interaction effects to the total number of markers; $N_{Q\cap Q\times E}/N_{\text{Marker}}$, proportion of the number of effects to the total number of markers; $H_Q$, proportion of the trait variance contributed by overall main effects; $H_{Q\times E}$, proportion of the trait variance contributed by the overall $Q \times E$ interaction effects

as the critical values. Permutation tests (Churchill and Doerge 1994) may be used to generate empirical critical values. We hesitated using permutation tests because they were originally proposed for interval mapping. For multiple QTL analysis, its suitability is questionable. We believe that the multiple QTL mapping may have already considered the multiple tests, since the test for each marker is conditioned on all other markers. Anyway, the fact that we did not use permutation tests does not mean that other people should not use the permutation tests to draw the critical values. Assume that permutation tests can be justified for multiple QTL mapping, they can be easily implemented with the proposed EM algorithm because of the fast speed. The fact that our EM algorithm is developed based on the hierarchical model (a hybrid between Bayesian and frequentist approaches), the asymptotic theory derived based on the frequentist approach may not apply to the hierarchical model. As a result, the test statistics may not follow the corresponding central distributions under the null models. Therefore, the permutation test for drawing the critical values of the test statistics may be an alternative way to decide the significance of a detected QTL effect. Permutation tests for multiple QTL mapping should be thoroughly investigated before they can be comfortably applied to this kind of multiple QTL models.

From genomic selection point of view, significance tests may not be required because all markers should be applied to predict the whole genome effect for each line, regardless how small their effects are (Meuwissen et al. 2001). Recently, genomic selection has become a hot topic for animal and plant breeding (Goddard and Hayes 2007, 2009; Goddard et al. 2010; Hayes et al. 2009; Heffner et al. 2009; Jannink et al. 2010; Meuwissen et al. 2001; Nielsen et al. 2009; Schaeffer 2006; Sonesson and Meuwissen 2009; Xu 2003; Xu and Hu 2010; Zhang et al. 2011). Genomic selection using multiple environmental data should be a useful subject for further investigation.

**Acknowledgments** We greatly appreciate two anonymous reviewers and the associated editor for their comments on an early version of the manuscript and their suggestions in revision of the manuscript. The project was supported by the USDA National Institute of Food and Agriculture Grant 2007-02784 to SX.

## References

Attari HE, Hayes P, Rebai A, Barrault G, Dechamp-Guillaume G, Sarrafi A (1998) Potential of doubled-haploid lines and localization of quantitative trait loci (QTL) for partial resistance to bacterial leaf streak (Xanthomonas campestris pv. hordei) in barley. TAG Theor Appli Genet 96:95–100

Che X, Xu S (2010) Significance test and genome selection in bayesian shrinkage analysis. Int J Plant Genomics. doi:10.11155/2010/893206

Chen X, Zhao F, Xu S (2010) Mapping environment-specific quantitative trait loci. Genetics 186:1053–1066

Churchill GA, Doerge RW (1994) Empirical threshold values for quantitative trait mapping. Genetics 138:963–971

Fang M, Jiang D, Pu LJ, Gao HJ, Ji P, Wang HY, Yang RQ (2008) Multitrait analysis of quantitative trait loci using Bayesian composite space approach. BMC Genet 9:48. doi:10.1186/1471-2156-9-48

Goddard M, Hayes B (2007) Genomic selection. J Anim Breed Genet 124:323–330

Goddard M, Hayes B (2009) Mapping genes for complex traits in domestic animals and their use in breeding programmes. Nat Rev Genet 10:381–391

Goddard M, Hayes B, Meuwissen T (2010) Genomic selection in livestock populations. Genetics Res 92:413–441

Haley C, Knott S (1992) A simple regression method for mapping quantitative trait loci in line crosses using flanking markers. Heredity 69:315–324

Han F, Ullrich S, Chiarat S, Menteur S, Jestin L, Sarrafi A, Hayes P, Jones B, Blake T, Wesenberg D, Kleinhofs A, Kilian A (1995) Mapping of beta glucan content and beta glucanase activity loci in barley grain and malt. Theor Appl Genet 91:921–927

Han F, Ullrich S, Kleinhofs A, Jones B, Hayes P, Wesenberg D (1997) Fine structure mapping of the barley chromosome-1 centromere region containing malting-quality QTLs. TAG Theor Appl Genet 95:903–910

Hayes P, Liu B, Knapp S, Chen F, Jones B, Blake T, Franckowiak J, Rasmusson D, Sorrells M, Ullrich S (1993) Quantitative trait locus effects and environmental interaction in a sample of North American barley germ plasm. Theor Appl Genet 87:392–401

Hayes B, Bowman P, Chamberlain A, Goddard M (2009) Genomic selection in dairy cattle: progress and challenges. J Dairy Sci 92:433–443

Heffner EL, Sorrells ME, Jannink JL (2009) Genomic selection for crop improvement. Crop Sci 49:1–12

Henderson C (1975) Best linear unbiased estimation and prediction under a selection model. Biometrics 31(2):423–447

Jannink JL, Lorenz AJ, Iwata H (2010) Genomic selection in plant breeding: from theory to practice. Brief Funct Genomics 9:166–177

Jiang C, Zeng ZB (1997) Mapping quantitative trait loci with dominant and missing markers in various crosses from two inbred lines. Genetica 101:47–58

Knapp S, Bridges W, Birkes D (1990) Mapping quantitative trait loci using molecular marker linkage maps. Theor Appl Genet 79:583–592

Meuwissen T, Hayes B, Goddard M (2001) Prediction of total genetic value using genome-wide dense marker maps. Genetics 157:1819–1829

Nielsen HM, Sonesson AK, Yazdi H, Meuwissen THE (2009) Comparison of accuracy of genome-wide and BLUP breeding value estimates in sib based aquaculture breeding schemes. Aquaculture 289:259–264

Piepho HP (2000) A mixed-model approach to mapping quantitative trait loci in barley on the basis of multiple environment data. Genetics 156:2043–2050

Romagosa I, Ullrich SE, Han F, Hayes PM (1996) Use of the additive main effects and multiplicative interaction model in QTL mapping for adaptation in barley. TAG Theor Appl Genet 93:30–37

Schaeffer L (2006) Strategy for applying genome wide selection in dairy cattle. J Anim Breed Genet 123:218–223

Sonesson AK, Meuwissen THE (2009) Testing strategies for genomic selection in aquaculture breeding programs. Genet Sel Evol 41:37

Tibshirani R (1996) Regression shrinkage and selection via the lasso. J Roy Stat Soc Ser B 58(1):267–288

Wald A (1943) Tests of statistical hypotheses concerning several parameters when the number of observations is large. Trans Am Math Soc 54:426–482

Xu S (2003) Estimating polygenic effects using markers of the entire genome. Genetics 163:789–801

Xu S (2007) Derivation of the shrinkage estimates of quantitative trait locus effects. Genetics 177:1255–1259

Xu S (2010) An expectation–maximization algorithm for the Lasso estimation of quantitative trait locus effects. Heredity 105:483–494

Xu S, Hu Z (2010) Methods of plant breeding in the genome era. Genet Res 92:423–441

Yi N, Xu S (2008) Bayesian LASSO for quantitative trait loci mapping. Genetics 179:1045–1055

Zhang Z, Zhang Q, Ding X (2011) Advances in genomic selection in domestic animals. Chin Sci Bull 56:2655–2663

# Genotype by Environment Interaction of Quantitative Traits: A Case Study in Barley

**Fuping Zhao[1] and Shizhong Xu[2]**
Department of Botany and Plant Sciences, University of California, Riverside, California 92521

**ABSTRACT** Genotype by environment interaction is a phenomenon that a better genotype in one environment may perform poorly in another environment. When the genotype refers to a quantitative trait locus (QTL), this phenomenon is called QTL by environment interaction, denoted by Q×E. Using a recently developed new Bayesian method and genome-wide marker information, we estimated and tested QTL main effects and Q×E interactions for a well-known barley dataset produced by the North American Barley Genome Mapping Project. This dataset contained seven quantitative traits collected from 145 doubled-haploid (DH) lines evaluated in multiple environments, which derived from a cross between two Canadian two-row barley lines, Harrington and TR306. Numerous main effects and Q×E interaction effects have been detected for all seven quantitative traits. However, main effects seem to be more important than the Q×E interaction effects for all seven traits examined. The number of main effects detected varied from 26 for the maturity trait to 75 for the heading trait, with an average of 61.86. The heading trait has the most detected effects, with a total of 98 (75 main, 29 Q×E). Among the 98 effects, 6 loci had both the main and Q×E effects. Among the total number of detected loci, on average, 78.5% of the loci show the main effects whereas 34.9% of the loci show Q×E interactions. Overall, we detected many loci with either the main or the Q×E effects, and the main effects appear to be more important than the Q×E interaction effects for all the seven traits. This means that most detected loci have a constant effect across environments. Another discovery from this analysis is that Q×E interaction occurs independently, regardless whether the locus has main effects.

**KEYWORDS**
barley
Markov chain Monte Carlo
mixed model
quantitative trait locus
Q×E interaction

Genotype by environment interaction is a phenomenon that genotype effects may significantly differ across environments. When the genotype refers to a quantitative trait locus (QTL), G×E interaction is renamed as QTL by environment interaction, denoted by Q×E. The magnitude of Q×E interaction for a particular locus is measured by the deviation of the estimated QTL effect in a specific environment from the average estimated QTL effect across environments. A QTL with a small Q×E interaction is more stable than a QTL with a larger Q×E interaction. A more stable QTL has a wider inference space and can be used in plant breeding across all environments. On the contrary, an unstable QTL can only be used in the environment from which it is detected.

Q×E interactions for quantitative traits in crops across multiple environments have been ubiquitous. Boer *et al.* (2007) reported that most of the detected QTL controlling grain yield and grain moisture of maize were influenced by temperature differences during critical stages of the growth. Li *et al.* (2010) found that several QTL governing growth trajectories of soybean cause significant genotype-environment interaction for plant height. Paterson *et al.* (2003) showed that genetic control of cotton fiber quality was markedly affected both by general difference between growing seasons and by specific differences in water management regimes. Yang *et al.* (2007) found that majority of the QTL detected for nine quantitative traits of wheat interact with drought stress and well-watered conditions. As for barley, G×E or Q×E interactions have been reported by several investigators (Cherif *et al.* 2010; Hayes *et al.* 1993; Piepho 2000; Tinker *et al.* 1996).

Three models have been proposed for detection of Q×E interaction. The simplest method is the standard two-way ANOVA (Pillen


doi: 10.1534/g3.112.002980
Manuscript received February 25, 2012; accepted for publication May 7, 2012

Supporting information is available online at http://www.g3journal.org/lookup/suppl/doi:10.1534/g3.112.002980/-/DC1
[1]Present address: Institute of Animal Sciences, Chinese Academy of Agricultural Sciences, Beijing 100193, China.
[2]Corresponding author: Department of Botany and Plant Sciences, University of California, Riverside, CA 92521. E-mail: shizhong.xu@ucr.edu

**Table 1 BIC scores of the five variance-covariance structures for the seven agronomic traits of barley in the Harrington×TR306 double haploid population**

| Covariance Structure | BIC | | | | | | |
|---|---|---|---|---|---|---|---|
| | Height | Heading | Kernel Weight | Lodging | Maturity | Test weight | Yield |
| Homogeneous | 20149.77 | 10284.11 | 15294.42 | 17855.92 | 7546.815 | 13379.04 | 38325.64 |
| Heterogeneous | 19298.47 | 9915.423 | 14940.67 | 16969.93 | 6613.732 | 12531.28 | 36940.23 |
| First-order factor | 19343.48 | 10081.89 | 14984.32 | 16890.66 | 6447.124 | 13059.46 | 37035.67 |
| Second-order factor | 19371.16 | 10289.86 | 15237.74 | 16905.9 | 6914.439 | 13630.45 | 37285.38 |
| Third-order factor | 19388.94 | 10289.82 | 15193.52 | 16925.5 | 6488.625 | 13144.99 | 37173.47 |

*et al.* 2003; Tinker and Mather 1995), in which Q×E interaction is tested one marker at a time. A slightly more advanced method is the split-plot ANOVA (Utz and Melchinger 1996; Utz *et al.* 2000), in which each genotype is considered to be a main plot, and observations from different environments play the role of split-plots. The common practice for Q×E analysis is to conduct interval mapping (Lander and Botstein 1989) or composite interval mapping (Zeng 1994) for each environment separately and then to compare the QTL mapping results for these environments (Li *et al.* 2007). If a QTL is detected in some environments but not in others, Q×E interaction is implied. This approach is subject to the same drawback as the ANOVA in terms of ignoring the covariance of the residuals because data are analyzed one environment at a time. Multivariate repeated measurement analysis is a more advanced method of Q×E analysis. Phenotypes of the same trait measured in different environments are treated as "different traits." This multivariate approach to QTL mapping was first proposed by Jiang and Zeng (1995). The advantage of this method is that the variance-covariance matrix of the residuals can be incorporated into the model. So far, only unstructured covariance matrix (full positive definite matrix) has been considered under the multivariate QTL mapping. Recently, Piepho (2005) proposed a mixed-model approach to modeling highly structured covariance matrix and showed that the mixed-model approach outperforms all the methods described above.

Chen *et al.* (2010) recently developed a new Bayesian shrinkage method for estimating and testing Q×E interactions. This method estimates all main effects and Q×E interactions simultaneously in a single model. When the number of environments is large, Chen *et al.* (2010) used the variance of the estimated QTL effects across multiple environments as a measure of the Q×E interaction. This approach has tremendously simplified Q×E studies. In addition, they incorporated the permutation analysis into the Q×E study and provided a significance

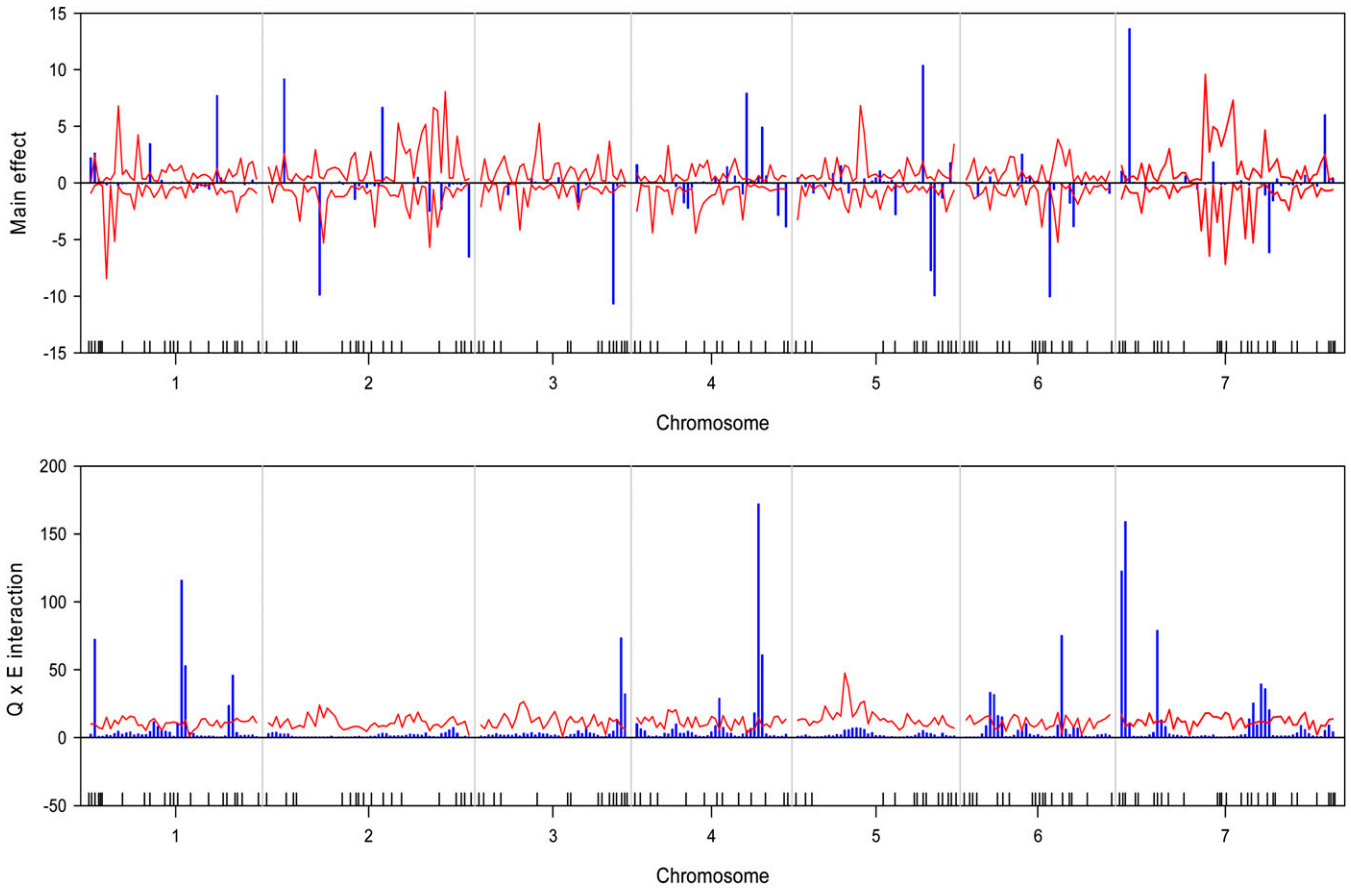


**Figure 1** Estimated main QTL effects (upper panel) and Q×E interaction effects (lower panel) across the barley genome for the yield trait. Chromosomes are separated by the vertical reference lines. The needles (in blue) represent the effects and the curves (in red) represent the 99% confidence intervals generated from a permutation analysis. The ticks on the horizontal axis indicate the marker positions.

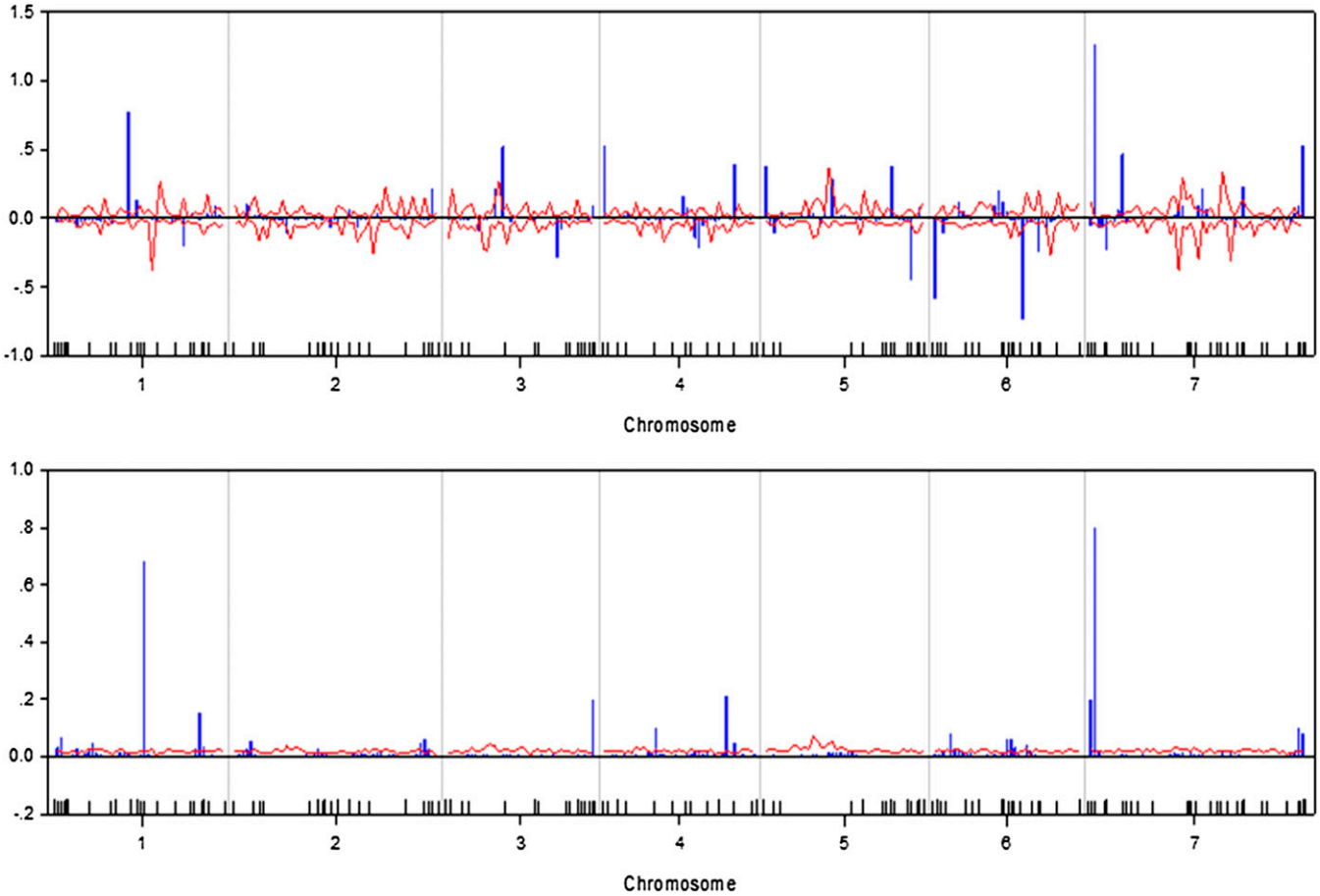


**Figure 2** Estimated main QTL effects (upper panel) and Q×E interaction effects (lower panel) across the barley genome for the test weight trait. Chromosomes are separated by the vertical reference lines. The needles (in blue) represent the effects and the curves (in red) represent the 99% confidence intervals generated from a permutation analysis. The ticks on the horizontal axis indicate the marker positions.

test for each effect. Chen *et al.* (2010) used the yield trait of barley as an example to demonstrate the application of the new method. Numerous main and Q×E study interaction effects were detected for that trait. This well-known barley data set was developed by the North American Barley Genome Mapping Project (Tinker *et al.* 1996). In the barley experiment, the investigators measured a total of seven quantitative traits from multiple environments and a total of 127 mapped markers that cover 1500 cM of the barley genome. Incorporating all 127 markers into a single model, Chen *et al.* (2010) only analyzed one of these traits. To capture the whole-genome marker information, we inserted a pseudo marker every 5 cM for a marker interval greater than 5 cM, and the total number of loci was 304. Then we analyzed all seven traits with 304 markers using the new method to draw general conclusions and reported the results in this study. As the genome coverage of the markers was quite high, no QTL would be missed. A general conclusion about the relative importance of Q×E in these quantitative traits is drawn, which can help us understand the genetic architecture of the complex quantitative traits to guide practical breeding programs of barley aimed at improving crop production in difficult environments.

## MATERIALS AND METHODS

### Experimental data

The data were retrieved from the North American Barley Genome Mapping Project (NABGMP) website (http://gnome.agrenv.mcgill.ca/). The experimental design and results were reported by Tinker *et al.* (1996). For the article to be self-contained, we briefly summarized the experiment here. This experiment consisted of a doubled haploid population with $n = 145$ lines derived from a cross between two Canadian two-row barley lines, Harrington and TR306. Seven traits were investigated in the project: yield, heading, maturity, height, lodging, kernel weight, and test weight. The 145 lines were grown in a range of environments: yield was measured in 28 environments, heading in 29, maturity in 15, height in 27, lodging in 17, kernel weight in 25, and test weight in 28 environments. A total of 127 mapped markers covered 1500 cM of the barley genome (seven chromosomes). The genotype of each marker was coded as $-1$ for the TR306 allele and +1 for the Harrington allele. A missing genotype was coded as 0. The data contained about ~4.9% missing marker genotypes and a few missing phenotypes.

We inserted a pseudo marker every 5 cM of the genome for a marker interval greater than 5 cM. Including the inserted pseudo markers, the total number of loci subject to analysis was 304. Missing marker and pseudo marker genotypes were inferred from flanking marker information using the multipoint method (Jiang and Zeng 1997). For example, the genotype indicator variable for line $j$ at marker $k$ is defined as

$$Z_{jk} = \begin{cases} +1 & \text{for } A_1A_1 \\ -1 & \text{for } A_2A_2 \end{cases} \quad (1)$$

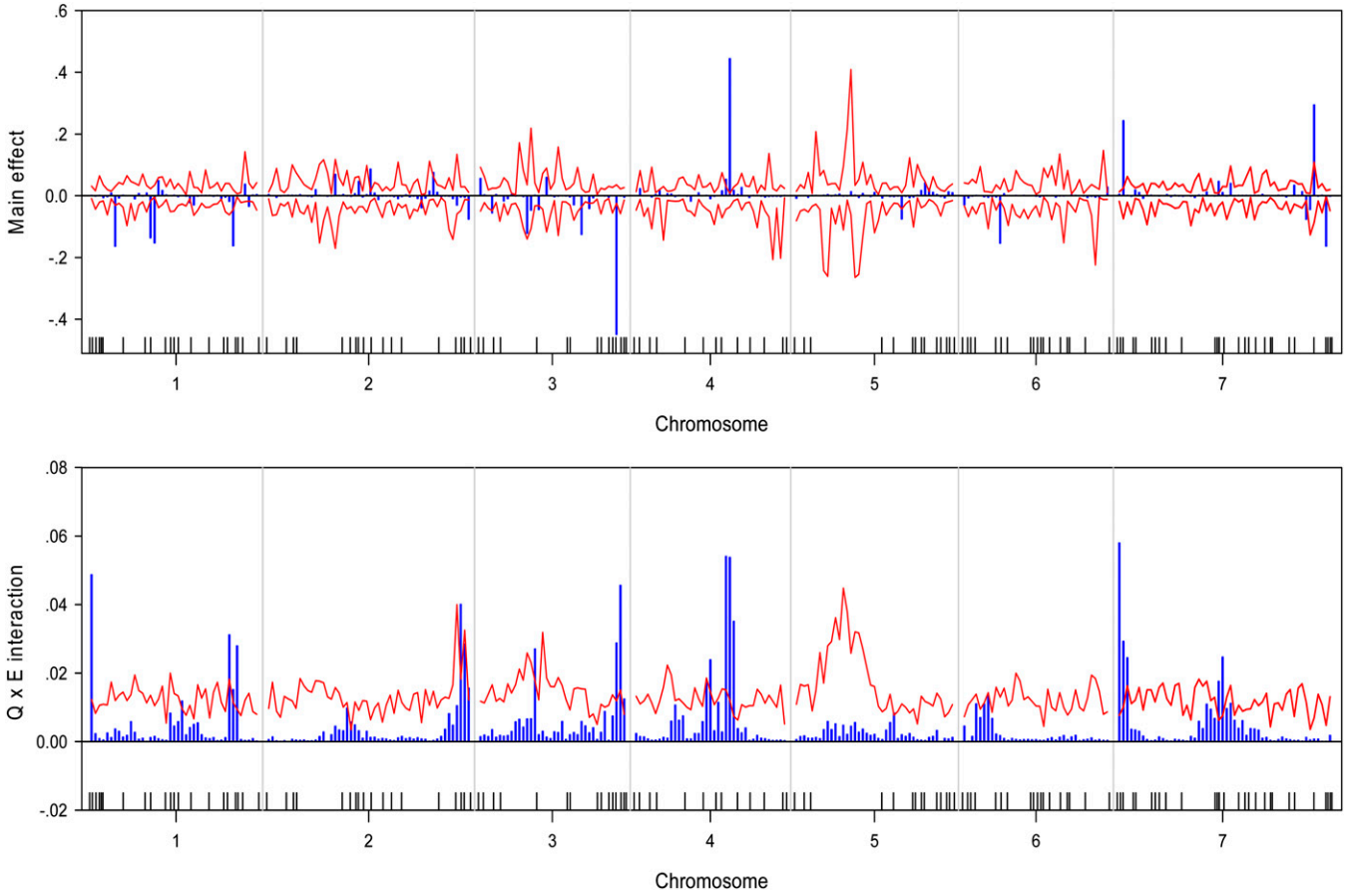


**Figure 3** Estimated main QTL effects (upper panel) and Q×E interaction effects (lower panel) across the barley genome for the maturity trait. Chromosomes are separated by the vertical reference lines. The needles (in blue) represent the effects and the curves (in red) represent the 99% confidence intervals generated from a permutation analysis. The ticks on the horizontal axis indicate the marker positions.

Let $p_{jk} = \Pr(Z_{jk} = 1|\text{marker})$ be the conditional probability of $Z_{jk} = 1$ inferred from all markers of the current chromosome. The conditional expectation for a missing $Z_{jk}$ is

$$E(Z_{jk}) = p_{jk} - (1 - p_{jk}) = 2p_{jk} - 1 \tag{2}$$

which will replace $Z_{jk}$ if $Z_{jk}$ is missing. It should be noted that each marker (true or pseudo) will be treated as a putative QTL in this research, *i.e.*, only the effects of markers (true and pseudo) will be estimated. If a QTL is located between two markers, its effect would be picked up by the two flanking markers. Hereafter, we use markers (including true and pseudo markers) and putative QTL interchangeably.

The missing phenotype $y_{ji}$ for line $j$ in the $i$th environment was drawn from the normal distribution with mean $\mu_i$ and variance $\sigma_i^2$, where $\mu_i$ is the average of phenotypes of all lines in the $i$th environment and $\sigma_i^2$ is the variance of phenotypes across lines in the $i$th environment. The seven traits were analyzed separately in seven analyses. The numbers of environments whose data contribute to the analysis for all traits are given in Table 2.

## Statistical method

Let $y_j = [y_{j1} \quad y_{j2} \quad \dots \quad y_{jm}]^{\mathrm{T}}$ be the phenotypic values for line $j$ collected in $m$ environments. The multivariate model for $y_j$ is

$$y_j = \beta + \sum_{k=1}^{p} Z_{jk}\gamma_k + \xi_j \tag{3}$$

where $\beta = [\beta_1 \quad \dots \quad \beta_m]^T$ is a vector of intercepts, $Z_{jk}$ is a numerically coded genotypic indicator variable for line $j$ at locus $k$, for $k = 1,\dots, p$, where $p = 304$ is the number of markers, including true and pseudo markers, $\gamma_k = [\gamma_{k1} \quad \gamma_{k2} \quad \dots \quad \gamma_{km}]^{\mathrm{T}}$ is an $m\times1$ vector of QTL effects for the $m$ environments and the residual error vector $\xi_j$ is assumed to be multivariate normal with density $p(\xi_j) = N(\xi_j|0,\theta)$, where $\theta$ is an $m\times m$ variance –covariance matrix. The variance- covariance structures of residual errors considered are identity, diagonal and factor analytic structured matrices.

For locus $k$, the mean of the marker effects cross the environments $\overline{\gamma}_k$ represents the main effects and the variance of the marker effects $\sigma_k^2$ represents the $Q\times E$ interaction. We used

$$\sigma_k^2 = \frac{1}{m}\sum_{i=1}^{m}(\gamma_{ki} - \overline{\gamma}_k)^2 \tag{4}$$

to represent the uniformity of the QTL effects cross environments. When there is no $Q\times E$ interaction, we expect that $\gamma_{k1} = \gamma_{k2} = \cdots = \gamma_{km}$ and thus $\sigma_k^2 = 0$. Since the method is a Bayesian method, prior and posterior distributions of parameters

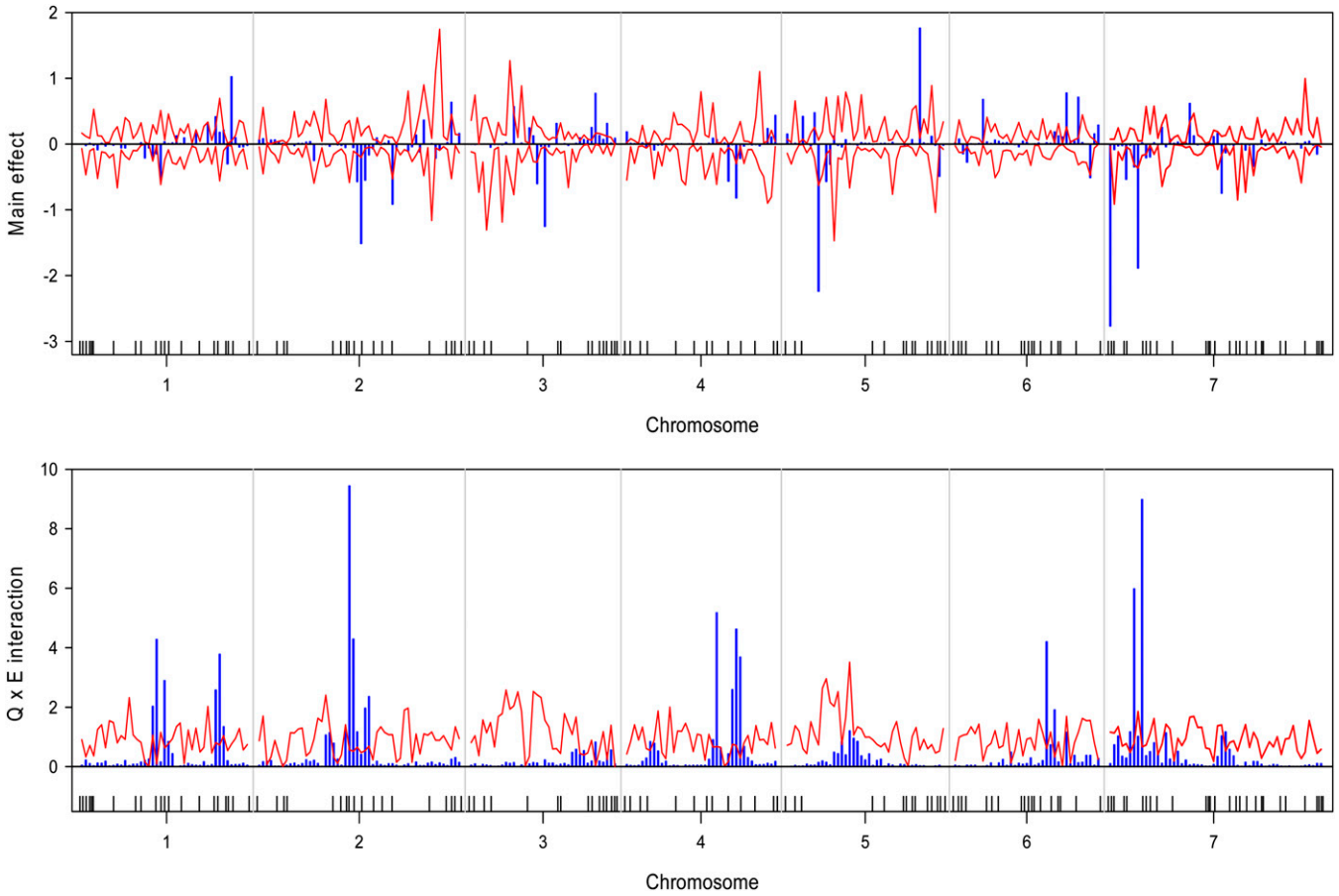


**Figure 4** Estimated main QTL effects (upper panel) and Q×E interaction effects (lower panel) across the barley genome for the lodging trait. Chromosomes are separated by the vertical reference lines. The needles (in blue) represent the effects and the curves (in red) represent the 99% confidence intervals generated from a permutation analysis. The ticks on the horizontal axis indicate the marker positions.

are required in the analysis. These distributions have been described in detail by Chen *et al.* (2010) and thus are not provided here in this report.

## MCMC sampling

The MCMC-implemented Bayesian analysis developed by Chen *et al.* (2010) was used for parameter estimation. The overall Markov chain contained 160,000 iterations. The first 40,000 iterations were deleted from the post MCMC analysis (burn-in deletion). Thereafter, the observations were saved in every 40 iterations to reduce the autocorrelation among different observations of the posterior samples. Therefore, the final posterior sample for analysis contained 3000 observations. Posterior means and other posterior statistics were obtained from the posterior sample of the 3000 observations.

## Model selection

We used five different variance-covariance structures to analyze the seven traits, which were (1) the homogeneous variance $\theta = I\sigma^2$, (2) the heterogeneous variance $\theta = D$, where $D = diag(d_1, \ldots, d_m)$ is a diagonal matrix with each diagonal element representing the residual error variance for the trait in that environment, (3) the first-order factor analytic structure $\theta = B_{m\times 1} \times B_{m\times 1}^T + D$, where $B$ is factor loading, (4) the second-order factor analytic structure $\theta = B_{m\times 2} \times B_{m\times 2}^T + D$, and (5) the third-order factor analytic structure $\theta = B_{m\times 3} \times B_{m\times 3}^T + D$. In order to select the optimal covariance structures for fitting the each trait, we used the Bayesian information criteria (BIC) to evaluate the performance of the five models. The BIC score was calculated using

$$\text{BIC} = -2\log(L) + p\log(n) \quad (5)$$

where $L$ is the likelihood function, $p$ is the number of parameters, and $n$ is the sample size. The BIC scores for the seven traits are shown in Table 1. As seen in Table 1, the minimum BIC scores of the lodging and maturity traits are under the first-order factor scenario and those of the remaining traits with the heterogeneous residual variance structure model reach the minimum values. These indicate that the first-order factor analytic model outperforms the other models for lodging and maturity traits and the heterogeneous residual variance structure model for the remaining traits. Therefore, we will analyze the lodging and maturity traits using the first-order factor analytic model and the remaining traits with heterogeneous residual variance structure model in the subsequent studies.

## Permutation test

To test the significance of the QTL effects, we conducted a permutation test to generate the null distribution of each main effect and each Q×E interaction. In the permutation analysis, we repeated the MCMC sampling method but randomly shuffled the phenotypes to artificially destroy the association between the markers and the phenotypes. This

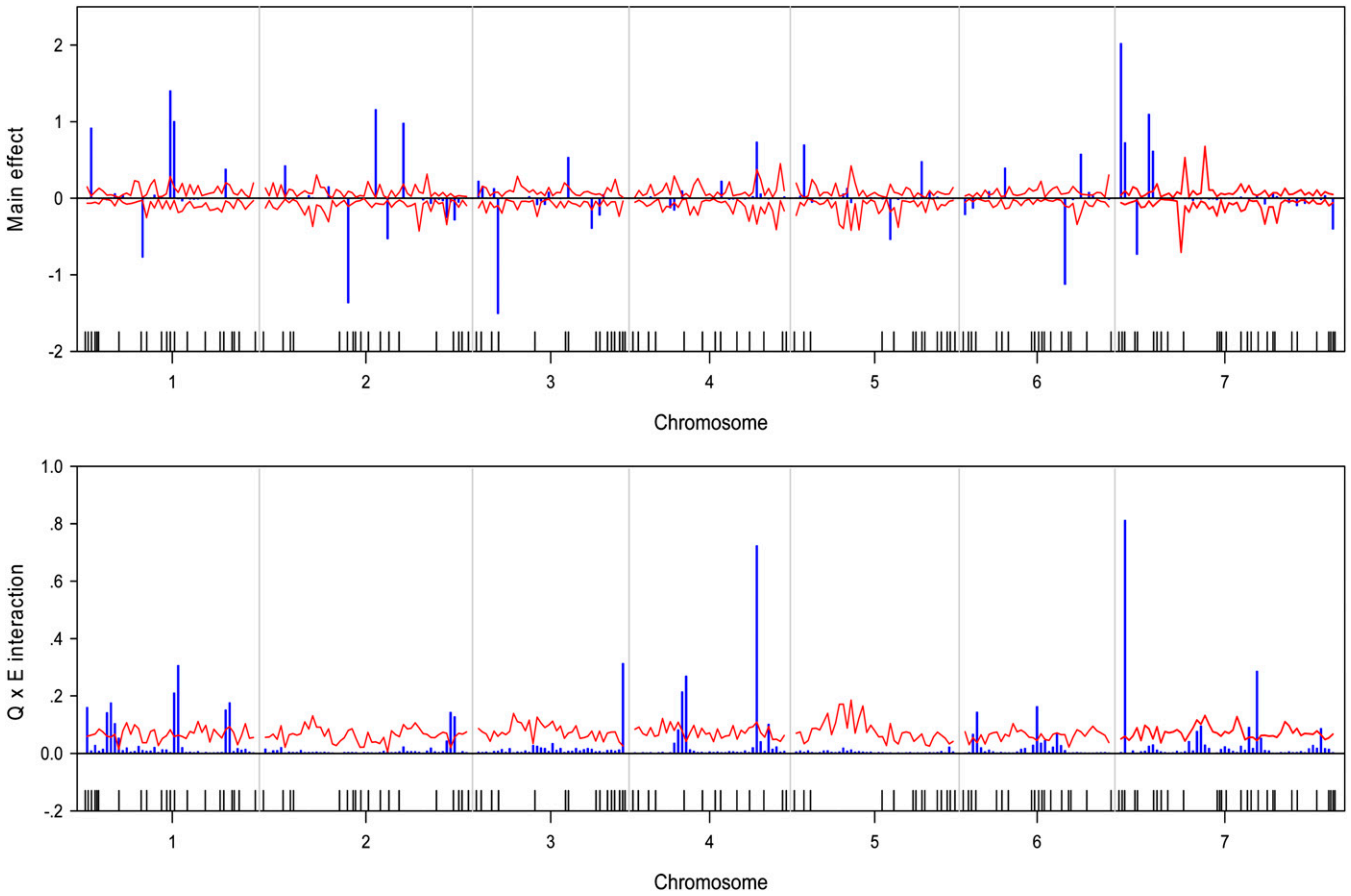


**Figure 5** Estimated main QTL effects (upper panel) and Q×E interaction effects (lower panel) across the barley genome for the kernel weight. Chromosomes are separated by the vertical reference lines. The needles (in blue) represent the effects and the curves (in red) represent the 99% confidence intervals generated from a permutation analysis. The ticks on the horizontal axis indicate the marker positions.

permutation test for Bayesian shrinkage analysis was proposed by Che and Xu (2010). We adopted this permutation analysis to draw the critical values for significance tests. The number of iterations for the permutation analysis was the same as that described for the original data analysis. The posterior distribution for each $\overline{\gamma}_k$ and $\sigma_k^2$ was inferred from the permuted posterior samples to draw the null distribution. An actual estimate of $\overline{\gamma}_k$ beyond the 0.5% and 99.5% interval indicates significant main effect while an actual estimate of $\sigma_k^2$ larger than the 99% of the null distribution indicates significant $Q \times E$ interaction.

## RESULTS

We wrote a SAS/IML program to implement the Bayesian analysis. The program took about 36∼54 CPU hours to complete the entire analysis for each trait on a Pentium PC with a 3.6-GHz processor and 3.00 GB RAM. The estimated QTL effect profiles, including the main effect and $Q \times E$ interaction, are depicted in Figure 1 for the trait yield. The figure also includes the 99% confidence interval profiles of the null distribution generated from the permutation analysis. The estimated QTL effect profiles for the remaining six traits are shown in Figure 2, Figure 3, Figure 4, Figure 5, Figure 6, and Figure 7. QTL main and interaction effects have been detected for each of the seven traits. However, no regions of the genome show evidence of a locus affecting all traits. One region near the end of the plus arm of chromosome 7 affected six traits (excluding heading), but the magnitudes of effects varied across traits. The results of this analysis are summarized in Table 1. The number of main effects varied from 26 (maturity) to 75 (heading) with an average of 61.86. Apparently, heading has the most detected effects with a total of 98 effects (75 main and 29 Q×E effects). Among the 98 effects, 6 loci had both the main and Q×E effects. Among the total number of detected loci, on average, 78.5% of the loci show the main effects, and 34.9% of the loci show Q×E interaction. This means that main effects contribute more of the genetic variance than the Q×E interaction effects. Other summary statistics can be found in the last column of Table 2. Overall, we detected many loci with either the main or the Q×E effects and the main effects appear to be more important than the Q×E interaction for all the seven traits. This means that most detected loci have a constant effect across environments. Another discovery from this analysis is that Q×E interaction occurs independently, regardless whether the locus has main effect or not. Traditional analysis that evaluates Q×E only on those loci that show significant main effects should be abandoned because that approach will fail to detect a large number of Q×E effects that show no main effects. Table 2 and Figures 1–7 give the summary of the discovery of this study. Detailed information regarding the actual estimated effects and locations of the significance loci are provided in the tables in File S1.

Responding to a reviewer's comment, we also used the mixed-model approach of Piepho (2005) to analyze these data for comparison. This method is single-point analysis. The linear model is

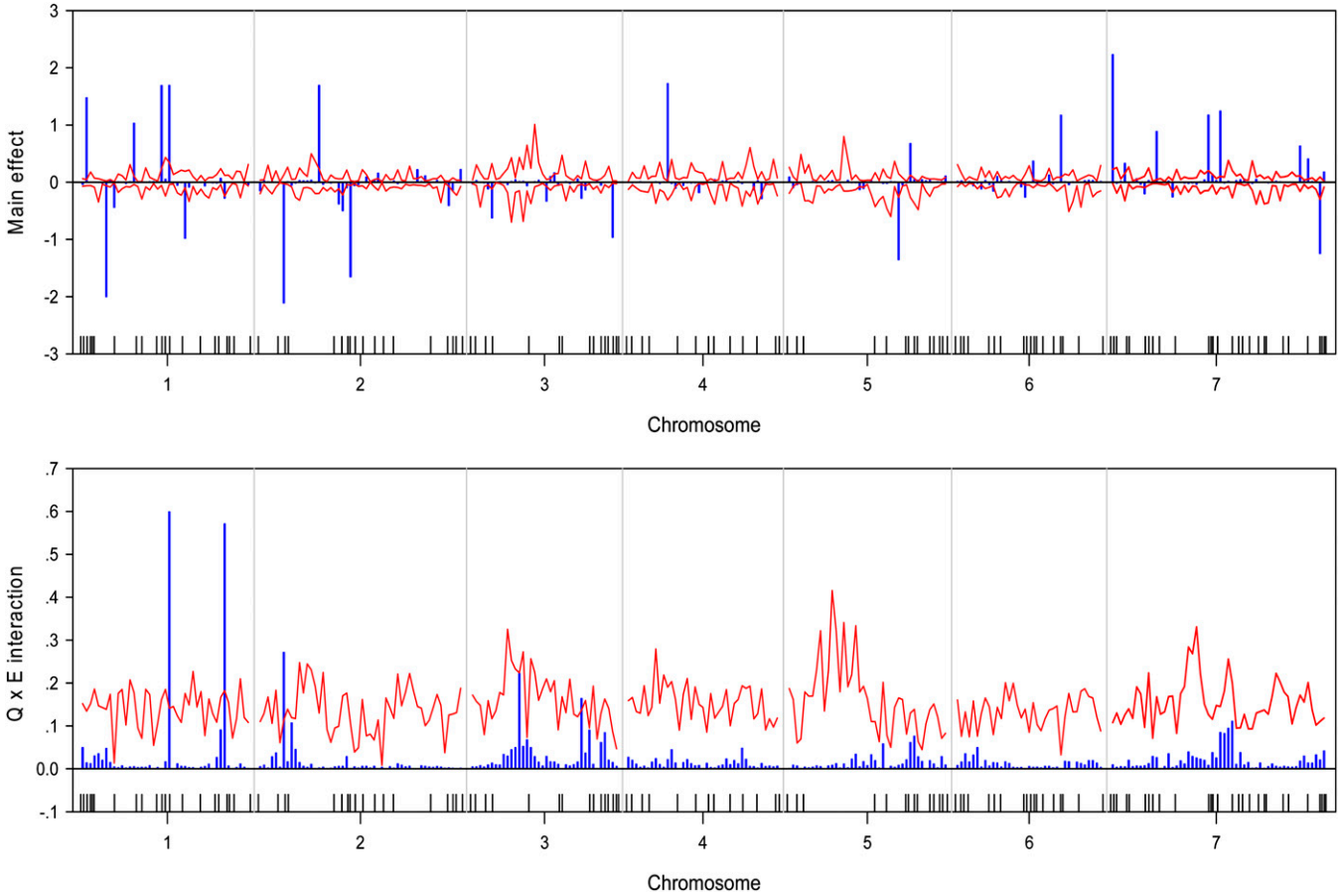


**Figure 6** Estimated main QTL effects (upper panel) and Q×E interaction effects (lower panel) across the barley genome for plant height. Chromosomes are separated by the vertical reference lines. The needles (in blue) represent the effects and the curves (in red) represent the 99% confidence intervals generated from a permutation analysis. The ticks on the horizontal axis indicate the marker positions.

$$y_{jm} = \mu_k + Z_{jk}\alpha_k + u_{km} + Z_{jk}a_{km} + e_{jm} \quad (6)$$

where $\mu_k$ is the general mean at the $k$th locus, $\alpha_k$ is the QTL main effect at the $k$th locus (treated as fixed effect), $u_{km}$ is the $m$th environmental main effect at the $k$th locus (treated as random), $a_{km}$ is the $Q \times E$ interaction effect in the $m$th environment at the $k$th locus (treated as random).

The mixed-model approach of Piepho (2005) was implemented using the MIXED procedure of the SAS system (SAS Institute, Cary, NC). As an example, we only presented in detail the result of the trait named yield. The estimated QTL main effects and Q×E interaction effects are depicted in Figure 8, where the top panel gives the estimated QTL main effects and the bottom panel shows the estimated Q×E interaction effects. This approach validated most of loci with QTL and Q×E interaction effects detected by the Bayesian analysis except a few places where the Bayesian analysis had extra peaks. For example, the two QTL with the effects in opposite directions in the middle of chromosome 2 detected by the Bayesian analysis disappeared in the mixed-model approach of Piepho (2005). Moreover, the magnitudes of the estimated QTL main effects and Q×E interaction effects are larger than those estimated by the Bayesian analysis. This comparison showed that the Bayesian analysis may be advantageous over the mixed-model approach. Note that this study is to report the Bayesian analysis of the barley data, not for the purpose of comparing different methods.

## DISCUSSION

We used the new Bayesian method developed by Chen *et al.* (2010) for Q×E interaction. In the original study, the authors used one trait (yield) as an example to demonstrate the method and test the computer program. In this study, we emphasize the application of this new method to Q×E detection for all seven traits measured in the experiment. This is an application study using an advanced statistical method. The 8 main effects and 18 Q×E interaction effects detected by Chen *et al.* (2010) for yield were all validated by this study. Furthermore, we detected more markers with main and Q×E interaction effects. The difference between the original study of Chen *et al.* (2010) and this study deserves further discussion. Chen *et al.* (2010) used 127 markers (all true markers), and they only estimated 127 main effects and 127 Q×E interaction effects. In this study, we used 304 markers (127 true markers and 177 pseudo markers) and estimated 304 main effects and 304 Q×E interaction effects. The additional effects we detected were largely contributed by the inserted pseudo markers. For example, many additional peaks that appeared in this study coincided with pseudo markers in large marker intervals. It was impossible for Chen *et al.* (2010) to detect these additional effects because they only analyzed the 127 true markers, not the 177 pseudo markers. Comparison of the yield trait between this study and that of Chen *et al.* (2010) clearly demonstrated the advantage of the pseudo marker insertion approach.

In the original barley QTL mapping experiment, the authors (Tinker *et al.* 1996) provided some preliminary results about Q×E

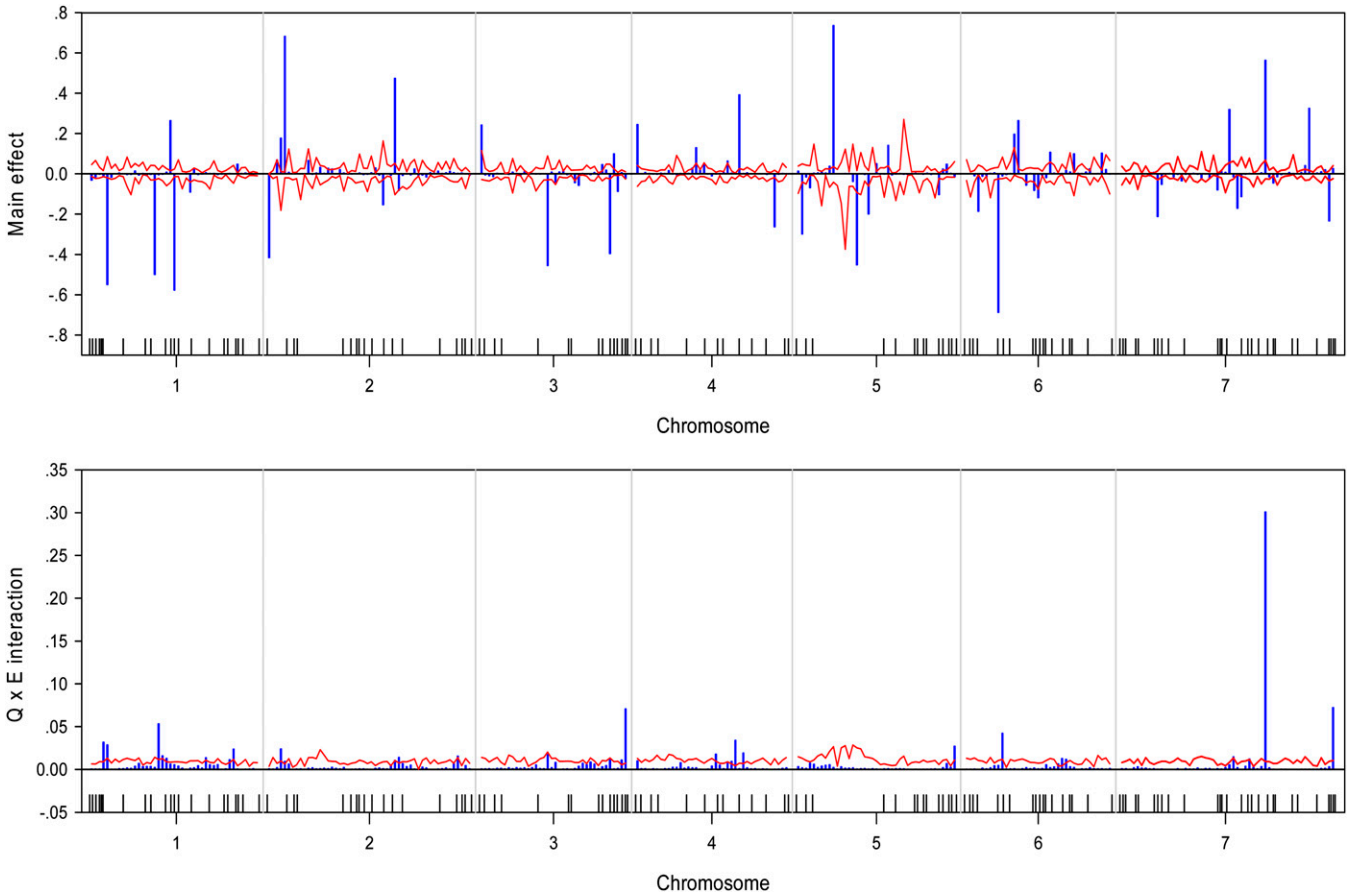


**Figure 7** Estimated main QTL effects (upper panel) and Q×E interaction effects (lower panel) across the barley genome for the date of heading. Chromosomes are separated by the vertical reference lines. The needles (in blue) represent the effects and the curves (in red) represent the 99% confidence intervals generated from a permutation analysis. The ticks on the horizontal axis indicate the marker positions.

interactions using the interval mapping (Lander and Botstein 1989) and composite interval mapping approaches (Zeng 1994). The difference between the interval mapping and the Bayesian mapping in the context of Q×E is that the Bayesian method uses a multivariate (multiple environments in this case) and multiple QTL model. All parameters and significance tests are performed simultaneously within the same model. Advantages of the simultaneous analysis over the one-environment-and-one-marker analysis are 3-fold: (a) conclusions are drawn from the result of the same analysis, rather than from separate analyses; (b) significance tests are conducted simultaneously in one experiment, and thus no adjustment is required regarding the experiment-wise Type I error rate; and (c) more effects can be detected using the joint analysis. We examined the Q×E interaction effects detected from the *ad hoc* interval mapping studies by the original authors of the barley experiment (Tinker *et al.* 1996) and found that almost all effects detected by Tinker *et al.* (1996) were also detected in this study. The comparison is summarized in Table 3. Note that the numbers of QTL main effects and Q×E effects were counted directly from Figure 2 of Tinker *et al.* (1996). In addition, we detected more Q×E effects (see the tables in File S1 for detailed information about the results).

In contrast to common Q×E studies (Boer *et al.* 2007; Cherif *et al.* 2010; Hayes *et al.* 1993; Jansen *et al.* 1995; Li *et al.* 2007, 2010; Paterson *et al.* 2003; Piepho 2000; Tinker and Mather 1995; Tinker *et al.* 1996; Yang *et al.* 2007) in which QTL effects from each environment are estimated and tested, here we used the variance (a single value) of the QTL effects across all environments as a measurement of Q×E interaction. The test is now based on a single value of variance for each locus. This automatically converts the traditional fixed-model analysis into a random model analysis because we are now estimating and testing a variance component. This random model treatment has eliminated many problems related to the fixed-model analysis. For example, there is little concern about model saturation (overfitting) under the random model framework. When the number of environments increases, the number of parameters to be tested remains the same because there is still only one variance $\sigma_k^2$ per locus.

In this research, we used the permutation tests proposed by Chen *et al.* (2010) for drawing the empirical critical values of the test statistics to decide the significance of the detected QTL effects. In theory, significance test are not required in Bayesian analysis. However, the purpose of this study was to evaluate the genome-wide QTL main effects and Q×E interaction effects. We expected that some estimated QTL main effects and Q×E interaction effects might be detected by chance and thus wanted to exclude the noisy effects. In addition, the Bayesian mapping of Chen *et al.* (2010) was developed based on a hierarchical model and it is a hybrid method between the Bayesian and the frequentist approaches. The asymptotic theory derived based on the frequentist approach may not apply to the hierarchical model. Therefore, we employed the permutation test to separate the true QTL from the spurious QTL.

**Table 2 Summary statistics for the seven agronomic traits of barley in the Harrington×TR306 double haploid population using Bayesian mapping**

| | Trait | | | | | | | |
|---|---|---|---|---|---|---|---|---|
| | Height | Heading | Kernel Weight | Lodging | Maturity | Test Weight | Yield | Average |
| $N_E$ | 27 | 29 | 25 | 17 | 15 | 28 | 28 | 24.12 |
| $N_Q$ | 72 | 75 | 51 | 73 | 26 | 73 | 63 | 61.86 |
| $N_{Q\times E}$ | 4 | 29 | 23 | 43 | 22 | 35 | 31 | 26.71 |
| $N_{Q\cap Q\times E}$ | 4 | 6 | 10 | 22 | 7 | 13 | 10 | 10.29 |
| $N_{Q\cup Q\times E}$ | 72 | 98 | 64 | 94 | 41 | 95 | 84 | 78.28 |
| $N_Q/N_{Q\cup Q\times E}$ | 1.0000 | 0.7653 | 0.7969 | 0.7766 | 0.6341 | 0.7684 | 0.7500 | 0.7845 |
| $N_{Q\times E}/N_{Q\cup Q\times E}$ | 0.0556 | 0.2959 | 0.3594 | 0.4574 | 0.5366 | 0.3684 | 0.3690 | 0.3489 |
| $N_Q/N_{MK}$ | 0.2368 | 0.2664 | 0.1678 | 0.2401 | 0.0855 | 0.2401 | 0.2072 | 0.2063 |
| $N_{Q\times E}/N_{MK}$ | 0.0132 | 0.0954 | 0.0757 | 0.1414 | 0.0724 | 0.1151 | 0.1020 | 0.0879 |
| $N_{Q\cup Q\times E}/N_{MK}$ | 0.2368 | 0.3224 | 0.2105 | 0.3092 | 0.1349 | 0.3125 | 0.2763 | 0.2575 |
| $M_Q$ | 2.23 | 0.74 | 2.02 | 2.77 | 0.4493 | 1.27 | 13.61 | 3.2985 |
| $M_{Q\times E}$ | 0.60 | 0.30 | 0.81 | 9.4343 | 0.06 | 0.90 | 171.88 | 26.28 |

$N_E$, number of environments; $N_Q$,number of main effects; $N_{Q\times E}$,number of Q×E effects; $N_{Q\cup Q\times E}$, total number of effects; $N_{Q\cap Q\times E}$, number of both effects (main and Q×E effects); $N_Q/N_{Q\cup Q\times E}$, proportion of the number of main effect over the total number of effects; $N_{Q\times E}/N_{Q\cup Q\times E}$, proportion of the number of Q×E effects over the total number of effects; $N_Q/N_{MK}$, proportion of the number of main effects over the total number of loci (pseudo and true markers) ($N_{MK}$ = 304); $N_{Q\times E}/N_{MK}$, proportion of the number of Q×E effects over the total number of loci;$N_{Q\cup Q\times E}/N_{MK}$, proportion of the number of effects over the total number of loci; $M_Q$, the absolutely value of the largest main effect; $M_{Q\times E}$, the absolute value of the largest Q×E effect.

Understanding the relative importance of Q×E interaction is useful in plant breeding. The way we formulated the Q×E interaction is unique because it is measured as a variance component. The variance across environments reflects the stability of a QTL, in which a larger variance indicates a lower stability of the QTL. From the breeding point of view, understanding Q×E interaction is important in marker-assisted selection and breeding. A QTL with less or no Q×E interaction can be utilized in a broad range of conditions, whereas QTL with

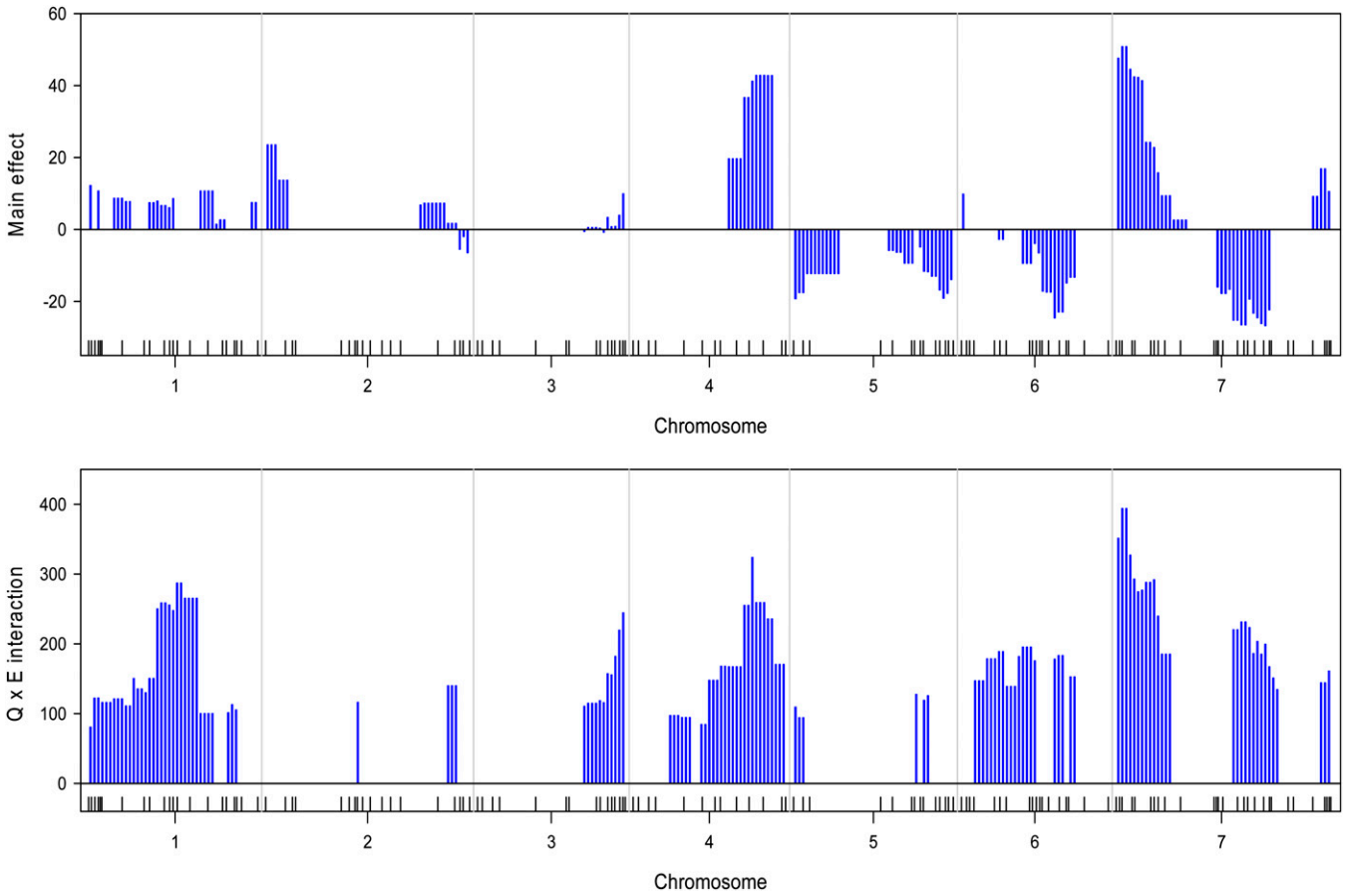


**Figure 8** Estimated main QTL effects (upper panel) and Q×E interaction effects (lower panel) across the barley genome for the yield trait using the mixed method approach of Piepho (2005). Chromosomes are separated by the vertical reference lines. The needles (in blue) represent the effects.

**Table 3 The numbers of QTL and Q×E interactions for the seven agronomic traits of barley in the Harrington×TR306 double haploid population detected by the interval mapping approach and validated by the Bayesian approach**

| Trait | Main Effect | | Q×E Interaction Effect | |
|---|---|---|---|---|
| | $N_{QD}$ | $N_{QV}$ | $N_{Q\times ED}$ | $N_{Q\times EV}$ |
| Height | 6 | 6 | 5 | 2 |
| Heading | 10 | 10 | 20 | 20 |
| Kernel weight | 6 | 6 | 18 | 16 |
| Lodging | 6 | 6 | 10 | 9 |
| Maturity | 4 | 4 | 5 | 4 |
| Test weight | 6 | 6 | 16 | 16 |
| Yield | 10 | 10 | 20 | 18 |

$N_{QD}$, number of QTL main effects detected using interval mapping by Tinker *et al.* (1996); $N_{QV}$, number of main effects validated using Bayesian mapping; $N_{Q\times ED}$, number of Q×E interaction effects detected using interval mapping by Tinker *et al.* (1996); $N_{Q\times EV}$, number of Q×E interaction effects validated using Bayesian mapping.

significant Q×E interaction can only be used in the specific environment in which it is detected.

## ACKNOWLEDGMENTS

We greatly thank two anonymous reviewers for their useful comments and suggestions on an earlier version of the manuscript. This project was supported by the Agriculture and Food Research Initiative of U.S. D.A. National Institute of Food and Agriculture 2007-02784 (to S.X.).

## LITERATURE CITED

Boer, M. P., D. Wright, L. Feng, D. W. Podlich, L. Luo *et al.*, 2007 A mixed-model quantitative trait loci (QTL) analysis for multiple-environment trial data using environmental covariables for QTL-by-environment interactions, with an example in maize. Genetics 177: 1801–1813.

Che, X., and S. Xu, 2010 Significance test and genome selection in Bayesian shrinkage analysis. Int. J. Plant Genomics 2010: Article ID 893206.

Chen, X., F. Zhao, and S. Xu, 2010 Mapping environment specific quantitative trait loci. Genetics 186: 1053–1066.

Cherif, M., S. Rezgui, P. Devaux, and M. Harrabi, 2010 Genotype × environment interactions and heritability of quantitative resistance to net blotch in Tunisian barley. Journal of Plant Breeding and Crop Science 2: 110–116.

Hayes, P., B. Liu, S. Knapp, F. Chen, B. Jones *et al.*, 1993 Quantitative trait locus effects and environmental interaction in a sample of North American barley germ plasm. Theor. Appl. Genet. 87: 392–401.

Jansen, R., J. Ooijen, P. Stam, C. Lister, and C. Dean, 1995 Genotype-by-environment interaction in genetic mapping of multiple quantitative trait loci. Theor. Appl. Genet. 91: 33–37.

Jiang, C., and Z. B. Zeng, 1995 Multiple trait analysis of genetic mapping for quantitative trait loci. Genetics 140: 1111–1127.

Jiang, C., and Z. B. Zeng, 1997 Mapping quantitative trait loci with dominant and missing markers in various crosses from two inbred lines. Genetica 101: 47–58.

Lander, E. S., and D. Botstein, 1989 Mapping Mendelian factors underlying quantitative traits using RFLP linkage maps. Genetics 121: 185–199.

Li, Q., Z. Huang, M. Xu, C. Wang, J. Gai *et al.*, 2010 Functional mapping of genotype-environment interactions for soybean growth by a semiparametric approach. Plant Methods 6: 13.

Li, Y., C. Wu, G. Jiang, L. Wang, and Y. He, 2007 Dynamic analyses of rice blast resistance for the assessment of genetic and environmental effects. Plant Breed. 126: 541–547.

Paterson, A., Y. Saranga, M. Menz, C. X. Jiang, and R. Wright, 2003 QTL analysis of genotype× environment interactions affecting cotton fiber quality. Theor. Appl. Genet. 106: 384–396.

Piepho, H. P., 2000 A mixed-model approach to mapping quantitative trait loci in barley on the basis of multiple environment data. Genetics 156: 2043–2050.

Piepho, H. P., 2005 Statistical tests for QTL and QTL-by-environment effects in segregating populations derived from line crosses. Theor. Appl. Genet. 110: 561–566.

Pillen, K., A. Zacharias, and J. Leon, 2003 Advanced backcross QTL analysis in barley (Hordeum vulgare L.). Theor. Appl. Genet. 107: 340–352.

Tinker N., and D. Mather, 1995 Methods for QTL analysis with progeny replicated in multiple environments. Journal of Agricultural Genomics 1. Available at: http://wheat.pw.usda.gov/jag/papers95/paper195/jqtl15.html.

Tinker, N., D. Mather, B. Rossnagel, K. Kasha, A. Kleinhofs *et al.*, 1996 Regions of the genome that affect agronomic performance in two-row barley. Crop Sci. 36: 1053–1062.

Utz, H., and A. Melchinger, 1996 PLABQTL: a program for composite interval mapping of QTL. Journal of Agricultural Genomics. Available at: http://wheat.pw.usda.gov/jag/papers96/paper196/indexp196.html.

Utz, H. F., A. E. Melchinger, and C. C. Schon, 2000 Bias and sampling error of the estimated proportion of genotypic variance explained by quantitative trait loci determined from experimental data in maize using cross validation and validation with independent samples. Genetics 154: 1839–1849.

Yang, D. L., R. L. Jing, X. P. Chang, and W. Li, 2007 Identification of quantitative trait loci and environmental interactions for accumulation and remobilization of water-soluble carbohydrates in wheat (Triticum aestivum L.) stems. Genetics 176: 571–584.

Zeng, Z. B., 1994 Precision mapping of quantitative trait loci. Genetics 136: 1457–1468.

*Communicating editor: B. S. Yandell*